The Possible Roles of CD73 and Adenosine in the Osteoimmunological Bone Resorption of Periradicular Periodontitis

The Possible Roles of CD73 and Adenosine in the Osteoimmunological Bone Resorption of Periradicular Periodontitis

A Thesis presented by:

Abdullah Abdulrahman Albassam, B.D.S

To

The Faculty of Medicine

In partial fulfillment of the requirements for the Degree of

Doctor of Medical Sciences

Research Mentor:

Toshihisa Kawai, D.D.S., Ph.D.

The Forsyth Institute

Harvard School of Dental Medicine

March 2016

Dedication

To my wife Aljohara, for her help, support, love, and patience during my DMSc journey.

To my little one, Hala who made our life meaningful.

To my Parents, Family for their endless support.

Acknowledgment

I would like to convey my sincere gratitude and thanks to my mentor Dr. Toshihisa Kawai. His dedication and devotion inspired me during my DMSc journey. I greatly admire and value everything I have learned from him, and I believe his effort will be a major contributor to my success and achievements in the future.

I would also like to extend my gratitude to Dr. Robert R. White for his support during my 5 years at Harvard School of Dental Medicine. His warm and fatherhood feelings made me feel home thousands of miles away from home.

Table of Contents

Abstract:

Introduction: Periradicular periodontitis is an inflammatory disease caused by perpetual microbial infection in the root canal system which, if left untreated, results in the destruction of tooth supporting tissues. Tenacious infection of virulent bacteria can lead to continuous activation of host immune response which results in excess production of proinflammatory mediators, including the bone resorption factor RANKL. To date, attempts to minimize the destruction of tooth supporting tissues have included laser therapy and phototherapy, but these approaches have been confined to treating and monitoring the exogenous etiology, i.e., bacterial infection. Therefore, to improve the diagnosis and treatment of periradicular periodontitis, new technologies are needed to control host cell biological responses and evaluate the level of inflammation in the root canal system and periradicular area.

Objectives: Intracellular generated adenosine triphosphate (ATP) and its metabolite, adenosine (ADO), act as major energy currencies in the cell system. Only recently has it been reported that extracellular ATP (eATP) released from activated neutrophils elicits proinflammatory responses, while ADO, which is generated via enzymatic conversion of ATP by cell surface-expressed ecto-5′-nucleotidase (CD73) and Ectonucleoside triphosphate diphosphohydrolase-1 (NTPDase1/CD39), functions as anti-inflammatory mediator. Accordingly, this study investigated the effects of CD73 and ADO on osteoimmunological bone resorption in periradicular periodontitis.

Methods: The possible anti-bone loss role of ADO was examined *in vitro* by reacting RANKL-stimulated RAW264.7 osteoclast precursors with ADO receptor agonist 5′-(N-Ethylcarboxamido) adenosine (NECA). More specifically, the effects of NECA on RANKL-induced osteoclastogenesis were evaluated by monitoring TRAP+ multinucleated cell number and pit formation. Since activated T cells are the major cellular source of RANKL in periradicular periodontitis, the effects of NECA on proliferation and sRANKL production by TCR/CD28-stimulated T cells were examined *in vitro*. The therapeutic efficacy of NECA on the pathogenic bone loss induced in periradicular periodontitis was evaluated in a pulp exposure-induced periradicular periodontitis model using C57BL/6 wild-type (WT) mice. On the other hand, the impact of ADO loss-of-function was compared between $CD73^{-/-}$Foxp3-$GFP^{+/+}$ mice and WT mice, both with experimentally induced periradicular lesion. Periradicular tissues were isolated from sacrificed mice, and the mRNAs of inflammation-associated and bone remodeling-related genes, amount of ATP and size of periradicular lesions were monitored up to 3 weeks using qPCR and μCT. Expressions of CD73 and other proteins in the periradicular tissues were examined by immunohistochemistry and immunofluorescence staining.

Results: As determined from the *in vitro* experiments, NECA significantly suppressed not only RANKL-mediated osteoclastogenesis from RAW264.7 cells *($P<0.05$)*, but also significantly downregulated proliferation and RANKL production from TCR/CD28-activated T cells *($P<0.05$)*, suggesting that the elicited signal could downregulate RANKL-induced osteoclastogenesis. As determined from the *in vivo*

experiments, the amount of ATP and expression of CD73 mRNA were significantly increased in the mouse periradicular lesion in a time-dependent manner. NECA-treated wild-type (WT) mice demonstrated significantly elevated mRNAs for CD39, CD73, alkaline phosphatase, and RUNX2, while showing decreased expressions of RANKL and IL1-β mRNAs, accompanied by diminished size of periradicular lesion, compared to nondrug-treated control WT mice experimentally induced with periradicular lesion. Finally, the amount of ATP and mRNAs for RANKL, IL1-β, IL-6, and TNF-α, as well as the size of periradicular lesion, were significantly larger *(P<0.05)* in $CD73^{-/-}$Foxp3-$GFP^{+/+}$ compared to control WT-mice.

Conclusion: By its catalytic action to convert ATP to ADO, increased CD73, by its catalytic action to convert ATP to ADO, in the periradicular lesion may play a role in downregulating inflammatory bone loss, suggesting the CD73/ADO axis as a novel therapeutic target for periradicular periodontitis, leading to the development of a therapeutic regime which, beyond controlling bacterial infection, can control host cell biological responses and, hence, the level of inflammation in the affected root apex.

Introduction

Periradicular periodontitis is an inflammatory disease that is caused by perpetual microbial infection in the root canal system, and it is usually followed by the destruction of the tooth supporting tissues, which include alveolar bone and periodontal ligament tissue. Failure of host response to eliminate virulent bacteria can lead to the over-activation of the host immune response resulting in excess production of proinflammatory mediators. In particular, RANKL produced by activated lymphocytes is the key cytokine that can induce bone loss in periradicular periodontitis by activation of osteoclasts. To date, several approaches have attempted to control host response and minimize destruction in the supporting tissues; however, such therapeutic approaches have been solely confined to treating the etiology, i.e., endodontic pathogens, in the root canal system. For the diagnosis and prognosis of periradicular periodontitis, a test to monitor the root canal infection of bacteria is practically employed. However, no methods have been developed to monitor biological responses, especially the level of inflammation, occurring in the periradicular lesion. In order to provide better diagnosis and prognosis of periradicular periodontitis, development of a non-biased monitoring system that reflects inflammatory status is sought.

ATP and its breakdown product adenosine (ADO) have been very well studied for their intracellular roles as the “energy currency” of cells. It is only very recently that these molecules have been recognized for their extracellular roles in regulating inflammatory processes. For example, extracellular ATP released from injured cells, or activated neutrophils, is causal for proinflammatory responses. More specifically, ATP released from activated neutrophils elicits a major endogenous danger signal via

ligation to the purinergic receptors, leading to the production of proinflammatory cytokines from surrounding leukocytes, such as T cells and macrophages that express P2X and P2Y receptors.

On the other hand, it was also revealed that eATP could be hydrolyzed to adenosine (ADO) by the ectonucleotidases CD39 and CD73, which are expressed on the surface of cells, including endothelial cells and lymphocytes. While eATP elicits proinflammatory responses, extracellular ADO (eADO) functions as an anti-inflammatory mediator, a key idea fundamental to the hypothesis supporting this proposal. It is known that ADO receptors, which have 4 isoforms, including A1, A_{2A}, A_{2B} and A3, are expressed in various organs and tissues. T cells express A_{2A} and A_{2B} receptors, which elicit inhibitory signals in activated effector T cells. Furthermore, chemical agonists for ADO receptors have been developed. Selective ligands of A1, A_{2A}, A_{2B} and A3 ADO receptors have shown potential in the treatment of numerous disorders in which inflammation is a feature.

In terms of the effects of extracellular purine nucleosides on osteoclast-mediated bone loss, ligation of P2Y nucleotide receptors appears to activate osteoclasts through NF-kB signaling, while agonists for adenosine receptors were reported to inhibit RANKL-mediated osteoclastogenesis. However, few studies have reported on the effects of extracellular adenosine on periradicular periodontitis. Since neutrophils are the major cellular infiltrates, following lymphocytes, in the periradicular lesion, it is conceivable that eATP levels increase in the periradicular tissues during the initial phase of immune-inflammatory response. However, as the disease state of periradicular lesion progresses, it has also been reported that the number of Foxp3+ T_{reg} cells

increases in the periradicular lesion induced in a mouse model, suggesting that Foxp3+ T_{reg} cells may participate in anti-inflammatory and anti-bone loss responses by conversion of ATP to ADO using CD73 expressed on their cell surface. In sum, this evidence suggests that the biological process of eATP may promote periradicular bone resorption, while elevation of the ADO concentration in local inflammatory lesion may suppress it. Thus, it would be worth investigating if eADO affects the production of RANKL by activated T cells or if eADO modulates RANKL-mediated osteoclastogenesis.

Therefore, the goals of this study are to 1) test the feasibility of ATP and ADO as biomarkers that reflect the status of proinflammatory and anti-inflammatory host responses in the periradicular lesion, respectively, and 2) examine if the approach to increase eADO can suppress the bone resorption induced in periradicular lesion.

Review of the literature:

Periradicular periodontitis:

Periradicular periodontitis is an inflammatory disease that is caused by persistent microbial infection in the root canal system, followed by the destruction of the tooth supporting tissues [1-3]. To reach the pulp and infect the root canal system, bacteria in the oral cavity have to pass through the dental hard structure. This can be achieved by caries, trauma, cracks, and rarely through lateral and apical foramina [4, 5]. Periradicular periodontitis occurs as a result of local inflammatory response, which is mediated by infiltrated inflammatory cells and their products [6, 7]. The inflammatory process ultimately results in periradicular bone resorption, which is the unique function of osteoclasts [8, 9]. Periradicular periodontitis is an outcome to endodontic infection and demonstrate itself as host defense response to pathogens emerging from the root canal system. It is viewed as a vigorous confronts between pathogenic factors and host defenses at periradicular area that result in local inflammatory response and resorption of periradicular tissues [10]. However, Once the root canal system has been properly cleaned and disinfected, Healing of the periradicular lesion and formation of new bone supporting tissue can begin [11]. Accordingly, Understanding the mechanisms of bone resorption and formation is crucial to the development of therapies for bone destructive diseases including periradicular periodontitis.

To date, several approaches have attempted to control host response and minimize destruction in the supporting tissues; however, such therapeutic approaches have been solely confined to treating the etiology, i.e., endodontic treatment. Meanwhile, no methods have been developed to monitor biological responses,

especially the level of inflammation, occurring in the periradicular lesion. In order to provide better diagnosis and prognosis of periradicular periodontitis, it would be desirable to develop a non-biased monitoring system that reflects inflammatory status in the pulp.

Periradicular immune response:

When the root canal system gets infected, various innate and adaptive immune cells release high amounts of inflammatory mediators. Basically, the innate immune response in the periradicular area can be manifested by the production of inflammatory cytokines and inflow of phagocytic leukocytes, most prominently polymorphonuclear leukocytes (PMNs) which play an important role as the first line of defense in periradicular periodontitis. Moreover, several studies showed that periradicular lesions composed of numerous and multiple types of inflammatory cells. These cells include T lymphocytes, B lymphocytes, macrophages, PMNs, plasma cells, mast cells, natural killer (NK), and dendritic cells [12-16]. Periradicular response can be considered as a duty of the immune system to confine and localize infections to prevent systemic dissemination [9, 17]. The innate immunity response to bacteria will influence and motivate the release of proinflammatory cytokines which is crucial for activation of adaptive immune response [18]. T- and B-cell-mediated adaptive immune responses will then act as protection from endodontic microbes, as well as develop bacterium-specific antibodies [7].

RANKL as possible mechanism of bone resorption process in periradicular periodontitis:

Receptor activator of NF-κB ligand (RANKL), osteoprotegerin (OPG) ligand (OPGL), and TNF-related activation-induced cytokine (TRANCE), are the most potent factors for inducing osteoclastogenesis [19, 20]. Prior to this discovery in the mid-1990s, consensus held that osteoclast development was regulated by factors expressed by "osteoblast/stromal cells", but no expectation was made that members of the TNF superfamily would be involved in bone remodeling [21]. RANKL is a member of the TNF cytokine family, and both membrane-bound (mRANKL) and soluble receptor activator of NF-kappaB ligand (sRANKL) are expressed in human T-cells, while the functional differences between the two remain unclear [22] The natural decoy receptor for RANKL is OPG, and osteoclast formation is regulated by the balance between OPG and RANKL [23]. The expression level of RANKL mRNA in human periradicular lesion is significantly higher than that of healthy periradicular tissue [24, 25], suggesting that locally produced RANKL is responsible for periradicular bone resorption. Nevertheless, the biological mechanism underlying such increase of RANKL in the periradicular lesion with attendant pathogenic bone resorption remains unclear. Therefore, investigating the pathophysiological mechanism causing periradicular lesions can lead the discovery of new novel therapies for periradicular periodontitis.

T_{regs} and its functions:

T_{regs} were formerly called suppressor T cells and were first reported in the early 1970s [26] and thought to be a special CD8+ subset. However, the old thought about this cell population was changed describing it as a minor population of CD4+ T cells

[27]. Subsequently, studies revealed that CD4+CD25+ T cells can suppress other cells and hypo-responsive at the same time [28]. T_{reg} can inhibit T cell response and prevent disease in many animal models [29] suppress both adaptive and innate immune response [30-32]. Other studies showed that CD4+CD25+ T_{reg} cells could suppress the proliferation of CD8+ and CD4+ T cells by its action independently of TGF-β and IL-10 cytokines. This was proven using T_{regs} derived from TGF-β and IL-10 deficient mice [29].

RANKL produced by T cells may be responsible for the osteoclast-mediated periradicular bone resorption:

Recent study using a mouse model of periradicular periodontitis demonstrated that CD3+ T lymphocytes produce RANKL in response to the bacteria infecting in the exposed dental pulp, which, in turn, results in the periradicular bone resorption [33]. More specifically, RANKL-positive T-cells, along with TARP+ osteoclasts, were identified in periradicular lesions induced in mice by pulp exposure. The commensal bacterium in mouse oral cavity, *Pasteurella Pneumotropica* (*P. pnumotropica(Pp)*), which was most often detected from inflamed exposed pulp, showed notably elevated serum IgG antibody response in pulp-exposed mice compared to control non-treated mice, indicating that the adaptive immune response is induced against *P. pnumotropica* after the pulp exposure. Very importantly, *Pp*-reactive T-cells isolated from *Pp*-immunized mice produced sRANKL in response to *ex vivo* exposure to *P. pneumotropica*. Therefore, as a result of adaptive immune response induced against bacteria infecting dental pulp, these results suggested that activated bacteria-reactive T

cells might cause periradicular bone resorption in a mouse model of periradicular periodontitis

In contrast to effector T cell subsets, such as, Th1, Th2 or Th17 cells, which mediate inflammatory responses, CD25+Foxp3+ regulatory T-cells (T_{reg}) play a pivotal role in downregulating the overactivation of Th1, Th2 or Th17 cells. In the context of marginal periodontitis, the incidence of CD4+CD25+ T_{reg} cells increase along with elevated levels of B-cells relative to T-cells, compared to healthy control gingival tissue or gingivitis tissue. Expressions of Foxp3+ (forkhead box P3), the key transcription factor controlling regulatory T-cells, anti-inflammatory cytokines, including TGF-β1, and IL-10, are more prominent in periodontitis than gingivitis or healthy control [34-36]. It was also reported that that CD4+CD25+Foxp3+ T_{reg} cells increased in periradicular lesions of human patients and that these T_{reg} cells expressed IL-10 and TGF-β. Human T_{reg} cells are also reported to suppress the proliferation of effector T-cells *in vitro,* in part by stimulating the production of IL-10 [37, 38]. These reports suggest that T_{reg} cells in both marginal and periradicular periodontitis may play regulatory roles in controlling local immune/inflammatory processes.

In the mouse model of periradicular periodontitis, the infiltration of Foxp3+ T_{reg} cells in the bone resorption lesion also increases [39]. Interestingly, T_{reg} infiltration into mouse periradicular lesion is delayed (days 7 to 14) compared to the infiltration of other effector immune cells, indicating that T_{reg} cells infiltrate as a counter-regulatory mechanism to attenuate overactive inflammatory response. These lines of evidence lead to the hypothesis that T_{reg} could help control the expansion of periradicular lesion, but such premise remains to be proven.

CD73 (Cluster of Differentiation 73):

CD 73 is a membrane-bound glycoprotein (ectoenzyme) expressed on many cell types including endothelial cells, subsets of T and B lymphocytes (mainly T_{regs}), and mesenchymal cells. This ectoenzyme is encoded by the NT5E gene in humans and Nt5e gene in mice. CD73 can hydrolyze Adenosine monophosphate (AMP) into adenosine. This adenosine can activate transmembrane ADO receptors and can function as either an anti-inflammatory or proinflammatory mediator. ADO also regulates permeability of the blood vessels endothelium and other hematological activities after an inflammatory stimulus.

CD73KO mice:

This knockout mouse was developed in 2004 by Linda F. Thompson, Oklahoma Medical Research Foundation, by targeting and replacing exon 3 of the 5' ecto-nucleotidase (Nt5e) gene at chromosome 9, thus eliminating the fraction of this ectoenzyme. These mice breed and gained weight normally, and they also have an intact immune system [40]. They exhibited increased edema in all organs except the brain, and increased vascular leakage under hypoxia. These KO mice show increased aggression toward humans as a behavioral phenotypic change. They can be used in the study of inflammatory and autoimmune diseases, as well as cancer and cardiovascular disorders.

The function of CD73 and CD39 in the immune system:

Recently, CD73 and CD39 have been further used as T_{regs} marker due to their high expression on the surface of Foxp3+ T_{regs} [41, 42]. Given the importance of both CD73 and CD39 in dephosphorylating the ATP to ADO and altering the ATP mediated proinflammatory status toward ADO-driven anti-inflammatory effects, they can both be viewed as “immunological switches” [43]. Also, a recent study showed that CD73 produced by T_{regs} downregulated the production of NF-κB through adenosine receptor A_{2A} and reduced the production of proinflammatory mediators [44].

With particular respect to innate immunity, elevation eATP levels can lead to activation of neutrophils, while elevated levels of eADO will lead to high production of anti-inflammatory mediators to prevent potential tissue injury [45]. Since neutrophils express both CD39 and CD73, These ectoenzymes are crucial in regulating and controlling extracellular purinergic activity to prevent inflammatory tissue injury caused by prolonged inflammatory response [46-48]. Moreover, macrophage activation and induction of proinflammatory cytokines such as IL-1β, IL-6, IL-18, and TNF-α are regulated by extracellular purine concentrations which are, in turn, regulated by CD39/CD73 axis [49-51]. A recent study showed that proinflammatory M1 macrophages reduced the amount of CD73 and CD39 which led to ATP accumulation and higher inflammatory response. On the contrary, M2 anti-inflammatory macrophages elevated the amount of CD73 and CD39, eventually increasing ADO levels leading to diminishing inflammatory response [52, 53].

Extracellular Adenosine and its four receptors:

Adenosine is formed from its precursor, adenosine triphosphate (ATP), in both intracellular and extracellular spaces. Adenosine triphosphate (ATP) and its breakdown product adenosine are very well studied in their intracellular roles as the "energy currency" of cells. It is only recently that these molecules have been recognized in their extracellular roles in regulating inflammatory processes. Metabolically stressful condition, such as hypoxia, ischemia and inflammation, can dramatically increase the extracellular purine nucleosides: ATP, ADP and adenosine [54]. It is well known that eATP can be hydrolyzed to adenosine (ADO) by ectonucleotidases CD39 (ENTPD1 [ectonucleoside triphosphate diphosphohydrolase-1]) and CD73 [55]. Diverse effects of extracellular purine nucleosides upon physiological process have now been characterized, including immune and inflammatory functions as discussed before.

Extracellular adenosine triphosphate (eATP) released from injured cells or activated neutrophils is causal for pro-inflammatory responses [56]. More specifically, ATP released from activated neutrophils elicits a major endogenous danger signal via ligation to the purinergic receptors P2X and P2Y, leading to the production of pro-inflammatory cytokines from surrounding leukocytes, such as T-cells and macrophages that express these receptors.

On the other hand, eADO binds to four different cell surface ADO receptors: A1, A_{2A}, A_{2B}, and A3. It is known that ADO receptors are expressed in various organs and tissues. T-cells express A_{2A} and A_{2B} receptors, which elicit inhibitory signals in the effector T cells [57]. Furthermore, chemical agonists for ADO receptors have been developed. Accordingly, selective ligands of A1, A_{2A}, A_{2B}, and A3 ADO receptors are

likely to be potent in the treatment of pain, arthritis, cancer and other disorders in which inflammation is a feature [58].

In terms of effects of extracellular purine nucleosides on osteoclast-mediated bone loss, ligation of P2Y nucleotide receptors (P2Y6 and P2Y7) appears to activate osteoclasts through NF-kB signaling [59, 60], while agonists for adenosine receptors were reported to inhibit RANKL-mediated osteoclastogenesis [61]. However, few studies in the literature have reported on the effects of eATP and eADO on periradicular periodontitis. Since neutrophils are the major cellular infiltrates following lymphocytes in the periradicular lesion [62], it is conceivable that the level of eATP increases in the periradicular tissue. However, the amount of ATP as well as ADO in the context of periradicular lesion has never been studied. In sum, these lines of evidence implicate a biological process in which eATP may promote periradicular bone resorption, while, at the same time, an elevated concentration of ADO in local inflammatory lesion may suppress it.

Extracellular Adenosine produced by T_{reg} cells may suppress periradicular periodontitis.

While production of anti-inflammatory cytokines, such as TGF-β and IL-10, from T_{reg} cells are implicated in the immunosuppressive mechanism mediated by T_{reg} cells, it remains unclear whether factors produced by T_{reg} cells can inhibit the inflammatory bone resorption in the periradicular lesion. Importantly, T_{regs} have been reported to induce tolerance in effectors T cells by eADO production based on their distinct expression of CD73 which converts eATP to adenosine [63, 64]. Indeed, considering

T_{reg} mediated immunosuppression, it appears that IL-10 production from T_{reg} cells seems to be required for ADO production, and that deficiency of ADO production from T_{reg} cells isolated from IL-10 KO mice results in the failure to inhibit contact hypersensitivity reaction [65]. Interestingly, it is totally unknown whether eADO affects the production of sRANKL by activated T-cells or if eADO modulates RANKL-mediated osteoclastogenesis. Collectively, therefore it is hypothesized that eADO produced by T_{reg} cells may play a role in the suppression of RANKL production in periradicular periodontitis

Specific Aims:

The interaction between pathogenic bacteria and local host immune response in the periradicular tissue with periradicular periodontitis leads to leukocyte infiltration composed of lymphocytes and neutrophils which, in turn, cause apical bone resorption and surrounding tissue destruction, partly by the production of proinflammatory cytokines RANKL. Recent study using a mouse model of periradicular periodontitis demonstrated that infiltration of Foxp3+ T regulatory (T_{reg}) cells in the periradicular lesion increases during the late stage of this disease, suggesting that T_{reg} cells downregulates' overreaction to the endodontic pathogens of which production of RANKL leads to the osteoclast-dependent bone loss in the periradicular lesion. However, it is unknown if 1) ATP produced from neutrophils in periradicular lesion can function as a proinflammatory mediator and 2) ADO converted from ATP by CD73 expressed on T_{reg} cells can, in turn, attenuate inflammatory bone resorption. Current therapeutic modalities treat the etiology of periradicular lesion, i.e., bacteria infiltrating the root canal system. In contrast, therapies that can directly affect host immune response are presently absent.

Hypothesis

It is hypothesized that eADO produced by CD73+Foxp3+ T_{reg} cells may play a role in suppressing the bone resorption induced in periradicular periodontitis.

This hypothesis was tested in the following three aims:

Specific Aim 1:

To investigate the effects of eADO produced from Foxp3+ T regulatory (T_{reg}) cells on the suppression of bone resorption induced in the course of periradicular periodontitis.

Specific Aim 2:

To determine if extracellular ADO produced by CD73+Foxp3+ T_{reg} cells can suppress RANKL production from TCR/CD28-stimulated T cells, which, in turn, down-regulate periradicular bone resorption.

Specific Aim 3:

To find an approach to increase eADO by administration of ADO receptor agonist as a possible adjunct to non-surgical root canal therapy.

Materials and methods:

All the materials, methods, and protocols used in this study were previously optimized in our lab or used according to the respective manufacturer's instructions.

In-vitro methods:

RANKL Mediated Osteoclastogenesis Assays:

Cells (RAW 264.7 cell line) were seeded in a 96 well plates (3000 cells/well) for TRAP staining assay and Corning® Osteo Assay Surface 24 well plates (Corning Life Sciences, catalog no. 3988XX1) (5000 cells/well) for pit formation assay. Minimum Essential Medium (MEM) Alpha (MEMα - Gibco) was used as a culture medium. The medium was supplemented with 10% FBS, 0.1 mM NEAA, 100 IU/ml penicillin and 100 µg/ml streptomycin. The plates were incubated in optimal conditions (37°C and 5% CO_2) for 24 hours. Cells were treated with different concentrations of ADO receptor agonists: NECA (potent non-selective adenosine receptor agonist with high affinity to A_{2B}), IB-MECA (Potent and selective A3 adenosine receptor agonist), and CCPA (Potent and selective adenosine A1 receptor agonist) ranging from 1 to 1000ng/ml in the presence of rRANKL 50 ng/ml (Propretech®). The media was replenished every 72 hours. After 6 days, when multinucleated osteoclast-like cells were observed, the cells were used for TRAP staining.

a. Tartrate Resistant Acid Phosphatase (TRAP) staining

In order to measure the mature osteoclasts differentiated from RAW264.7 cells when stimulated with RANKL in the presence or absence of the different ADO receptors agonists used in the experiment, differentiated osteoclasts were identified as TRAP+

multinuclear cells. RAW264.7 cells cultured for 6 days were fixed (5% formalin-saline) then stained for TRAP using a TRAP-staining kit, following the manufacturer's protocol (Sigma, St. Louis, MO). Nuclear counter staining was done using methyl green staining. The plates were then washed, dried and viewed using the EVOS XL digital inverted phase contrast microscope (Advanced Microscopy Group, Bothell, WA, USA). TRAP+ cells containing more than 3 nuclei (multinuclear) were counted using 20X objectives.

b. Pit formation assay

RAW264.7 cells cultured on Osteo Assay surface plates were incubated in 100 µl/well of 10% bleach (NaOCL) for 5 minutes to facilitate cell detachment from the plate surface. The plates were then washed with water and dried. Photomicrographs were captured using EVOS XL microscope. The captured digital image was transferred and saved in Adobe Photoshop CS5 software (Adobe Systems, San Jose, CA). Briefly, Images were captured in five areas using 20X objective. They were transferred to imaging software and areas of pitting were measured and represented in mm^2.

RANKL production by activated T-cells:

a. T-cells isolation and culture

T-cells were isolated from the spleen and cervical lymph nodes of wild-type C57BL/6J mice via negative selection using MACS beads (MACS Pan T cell isolation kit, Miltenyi Biotec, Auburn, CA, USA). The resulting enriched T-cell suspension showed more than 95% of CD3+ T-cells as analyzed by flow cytometry cell sorting. The isolated T-cells (2×10^5 cells/well) were stimulated with plate-bound anti-mouse β-TCR antibody and anti-mouse CD28 antibody (BD Biosciences) with or without NECA treatment. The

supernatant was collected after 48 hours of T-cell stimulation and saved for sRANKL ELISA.

b. ELISA

sRANKL levels in T-cells culture supernatants were determined using commercially available ELISA kits (R&D Systems, Inc., Minneapolis, MN, USA).

c. Thymidine incorporation assay

This assay employs an approach whereby 3H-thymidine (radioactive nucleoside) is incorporated into newly formed strands of DNA chromosomes throughout mitotic cell division. A scintillation beta-counter is used to detect and measure incorporation and radioactivity of a radiolabeled DNA strands with 3H-thymidine produced during cell mitosis.

In-vivo methods:

Animals:

Black wild-type (WT) mice (C57BL/6J) and CD73-/-Foxp3-GFP+/+ (C57BL/6J-background) mice were used in this study (8 weeks; body weight 25-30 g). WT mice were obtained from Jackson Laboratory (Bar Harbor, Maine, USA) and CD73-/-Foxp3-GFP+/+ congenic mice were generated in Dr. Kawai's lab by cross mating Foxp3-GFP+/+ and CD73-/- mice until reaching the homozygous targeted genes. Animals were housed at the Forsyth animal facility in cages having filtered air circulation system in order to maintain a specific pathogen free (SPF) environment. Temperature was kept at 70 +/- 5 degrees Fahrenheit and 50 +/- 20% relative humidity. A 12-hour light/dark cycle was maintained. Animals were fed with a standard rodent chow. The Institutional Animal

Care and Use Committee (IACUC) approved all procedures used in this study at the Forsyth Institute prior to all experiments.

Development of $CD73^{-/-}$Foxp3-$GFP^{+/+}$ congenic mice:

$CD73^{-/-}$ mice were generously donated by Dr. Linda Thompson from Department of Microbiology & Immunology, University of Oklahoma Health Sciences Center. $CD73^{-/-}$ Foxp3-$GFP^{+/+}$ congenic mice were generated by crossing $CD73^{-/-}$ mice with Foxp3-$GFP^{+/+}$ mice in the animal facility at the Forsyth institute. The primers sequences for genotyping were as the following:

$CD73^{-/-}$ 1: GCT ACT TCC ATT TGT CAC GTC C

$CD73^{-/-}$ 2: GTT TTG ATG CGT TCT GCA AG

$CD73^{-/-}$ 3: TAC CGT TGG CTG ACC TTT GT

Foxp3 KI-F: CAC CTA TGC CAC CCT TAT CC

Foxp3 KI-R: ATT GTG GGT CAA GGG GAA G

Induction of periradicular lesion:

Periradicular lesions were initiated by pulp exposure of the mandibular first molar pulp of 8-week-old C57BL/6J mice or $CD73^{-/-}$Foxp3-$GFP^{+/+}$ mice (C57BL/6J background). Mice were anesthetized by intraperitoneal injection of Ketamine HCl (80 mg/kg of body weight) and Xylazine (10 mg/kg) in sterile phosphate-buffered saline (PBS). Anesthetized mice were mounted on a jaw retraction board, and the operation was carried out under a surgical microscope (model MC-M92; Seiler, St. Louis, MO). All lower first molar pulps were exposed to the oral environment by means of a #1/4 round bur as described by Wang and Stashenko [9]. The exposure size was approximately

equivalent to the diameter of the bur. The pulp chamber was opened until the orifice of the canals could be visualized and probed with a No. 6 endodontic K file. Exposed teeth were left exposed to the oral environment during the entire experiment. Mice without pulp exposure were used as a negative control in each group.

Bacteria:

Pasteurella Pneumotropica (Pp) is a commensal mouse oral cavity bacterium, which is phylogenically closely related to *Aggregatibacter actinomycetemcomitans*, a human pathogen for localized aggressive periodontitis. It was reported that immune response against this microorganism elicits periodontal bone loss based on the RANKL expression from activated T cells [66]. Bacteria located in the exposed pulp were collected using paper points (Tulsa Dental Supply, USA) to confirm the colonization of *Pp* in root canal, followed by the cultured on *Pp* selection agar that contains vancomycin and bacitracin at 37ºC in CO_2 incubator. The results of this protocol produced a reproducible infection of the root canal system.

Systemic administration of ADO receptor agonist (NECA):

Systemic administration of non-selective adenosine receptor agonist NECA (Sigma-Aldrich, St. Louis, MO) began on the day of pulp exposure by 0.1mg/kg/day, i.p. injuction (n=5/group) in the gain-of-function experiment. The other group in this experiment received i.p. injections of PBS in the same volume (n=5/group) to standardize the stress levels induced during injections and minimize any confounding factors.

Sample preparation:

WT and CD73$^{-/-}$Foxp3-GFP$^{+/+}$ mice were randomly assigned into 4 different time point groups (n=15/group). Three groups received pulp exposure at the first molars (both left and right) of mandibular jaw. Mice were sacrificed at 7, 14 and 21 days from the pulp exposure. Control non-treated mice represented day 0. Mandibular jaws were collected from the mice sacrificed at the respective time points (0, 7, 14 and 21 days) for morphologic, histologic and molecular evaluation. The mandible was hemisected and the left side mandibular jaw was immediately frozen at −70°C for ATP detection and RNA extraction. The right side of the mandible was defleshed, rinsed with PBS and fixed in 4% paraformaldehyde solution over-night. After extensive washing under running water for 1 to 3 hours, the fixed jaw was subjected to micro-computed tomography (μCT) prior to decalcification and histological evaluation. Spleen and cervical lymph nodes were also isolated from mice after the sacrifice at each time point.

Assessment of the bone destruction:

Evaluation of periradicular bone resorption using a micro-computed tomography (μCT) was done following the protocol published by Balto et al. [67]. The fixed right side hemimandibular samples from C57BL/6 wild type mice and CD73$^{-/-}$Foxp3-GFP$^{+/+}$ mice were analyzed using a compact fan-beam-type tomograph optical computed-tomography (μCT40, Scanco Medical AG, Basserdorf, Switzerland) at the Forsyth microCT core. The μCT system provides a 10 μm nominal resolution. The imaging parameters were as follows: Tube voltage 70 kVp; current 140 mA; and integration time 300 ms. For each sample, approximately 150 micro-tomographic slices with an increment of 17 μm, covering the entire width of the hemimandible. The data were

exported into DICOM format and resliced following a standardized protocol using ImageJ® to obtain pivotal sections which included the crown and distal roots. Coronal pictures showing patent distal root canal apex were selected and exported in JPEG format. In order to quantify the two-dimensional aspect of periradicular bone resorption area, a standard template was applied on all pictures. The periradicular area was measured using Adobe Photoshop CS5 (Adobe Systems, San Jose, CA). Results of two-dimensional aspect of periradicular bone resorption area were expressed in square millimeters (mm^2).

Histological sample preparation:

After acquiring the μCT images, the right side of WT and $CD73^{-/-}$Foxp3-$GFP^{+/+}$ mice hemimandibles were decalcified using 10% ethylenediaminetetraacetic acid (EDTA) for 14 days in 4ºC temperature cold room over test tube rocker. EDTA solution was replenished every other day. The samples were then embedded in paraffin or frozen OCT compound (Tissue-Tek®, Sakura Finetek USA inc) for Immunohistochemical and immunofluorescence staining, respectively.

Immunohistochemical staining:

Paraffin embedded samples of WT and $CD73^{-/-}$Foxp3-$GFP^{+/+}$ mice were cut into serial sections at 6 μm thickness; every fifth sample was mounted and stained with Hematoxylin and Eosin (H&E) for morphological evaluation. Sections showing the region of interest (mesial and distal roots with periradicular lesion) were then selected and mounted.

Immunofluorescent Laser-Scanning confocal microscopy:

Frozen tissue sections embedded in OCT compound were cut (8 μm thickness) using a cryostat. Sections showing the region of interest (mesial and distal roots with periradicular lesion) were then mounted and kept at a temperature of -20°C. When needed, sections were washed with 0.5% bovine serum albumin (BSA), blocked with 5% BSA and left in humid chamber for 1 hour. Slides were then washed with 0.5% BSA and reacted with primary antibodies. Otherwise, control nonimmunized rabbit or goat IgG was used as a negative control. Primary antibodies were incubated in humid chamber at 4°C for overnight. On the following day, after washing the slides with 0.5% BSA, appropriate secondary antibodies were applied, respectively, and incubated for 2 hours in dark humid chamber at room temperature. Next, slides were washed with 0.5% BSA and subjected to counter nuclear staining. Mounting solution for immunofluorescent staining (Fluoromount G) was applied to place cover glass on the slide. Fluorescent images were captured by 0.3 um sequential optical sectioning using a confocal microscope (Zeiss LSM 780).

TRAP staining for osteoclasts in periradicular bone:

In order to identify the presence of osteoclast cells in the periradicular tissues of mice, paraffin embedded sections of both WT and $CD73^{-/-}$Foxp3-$GFP^{+/+}$ mice were stained using a TRAP staining kit following manufacturer protocol (Sigma, St. Louis, MO), followed by nuclear counterstaining with hematoxylin.

ATP detection and levels in the periradicular lesions:

In order to monitor the kinetics of eATP, isolated samples were prepared for the bioluminescence assay for quantitative detection of ATP. The tissue samples were homogenized and crushed in a 200 µl of PBS using mortar and pestle. Ten µl of this homogenized tissue sample were added to 100 µl of the reaction reagents (containing 0.5 mM D-luciferin, 1.25 µg/mL firefly luciferase, 25 mM Tricine buffer, pH 7.8, 5 mM MgSO4 , 100 µM EDTA and 1 mM DTT) and compared to the manufacturer's standard. The total volume in each well of the Optilux Black/Clear Flat Bottom plate was 110µl. Plate luminescence was measured after a 15-minute incubation period using the Synergy™ HT Multi-Mode Microplate Reader.

mRNA extraction from bone using a high speed homogenizer

Fresh samples of left side hemimandible were rinsed in PBS. The periradicular tissues surrounding the mesial and distal root apices were carefully extracted together with surrounding bone, in a block specimen under a surgical microscope. Periradicular tissues were rinsed in PBS, freed of clots, weighed, and immediately frozen at −70°C. The frozen sample was transferred to a pre-cooled Lysing matrix A tubes (MP Biomedical, Santa Ana, CA) containing 1 ml Trizol® reagent (Invitrogen, Carlsbad, CA). The contents in the tube were disrupted using a high speed homogenizer, FastPrep®-24 Instrument (MP Biomedical), for 30 seconds for 2 cycles with flakes of dry ice to maintain the temperature inside the homogenizer. After addition of chloroform (20% of total volume), the samples were centrifuged then transferred to RNA isolation tube (Phase-lock gel tube; 5 prime) and subjected to centrifugation for 5 minutes. The separated clear aqueous phase solution that contains RNA was mixed 1:1 with

isopropanol 99.5% (RNA/DNA-free) to separated RNA as insoluble component. After RNA dehydration and precipitation, separated RNA was washed with 70% ethanol. The resulting RNA pellet was air-dried and resuspended in DNA free water. The mixture was then treated with Turbo DNase™ (Ambion) to completely digest any DNA contamination following manufacture protocol. RNA samples were then tested for purity and quantified using Nanodrop 2000c spectrophotometers (Thermo Scientific, Cambridge, MA). Only samples that showed 260/280 ratios of 1.8-2.2 were used for qPCR.

Quantitative polymerase chain reaction (qPCR)

Complimentary DNA (cDNA) was synthesized using 1 µg of total RNA using iScript® cDNA synthesis kit (Bio-Rad Laboratories, Hercules, CA) by addition of reverse transcriptase (0.5 µl) in a total 20 µl of solution. qPCR was performed using LightCycler® 480 system (Roche applied science, Penzberg, Germany) with LightCycler 480 Sybr 1 master mix (Roche) for 50 cycles. The PCR cycling profile, as shown in the Roche manual and following the manufacturer's instructions for primers, consisted of an initial denaturation step at 95°C for 5 min, followed by 50 cycles of denaturation at 95°C for 15s, and annealing/extension 58-60°C for 60s. Melting Curve analysis was also performed using a single cycle of 95°C for 20s; 60°C for 20s; 40°C for 1s and 95°C prior to the final cooling.

The primers that were used during this experiment are:

Name	Source	Size(bp)	Forward Sequence 5'-3'	Reverse Sequence 5'-3'
Actb	Real time primers	160	AAGAGCTATGAGCTGCCTGA	TACGGATGTCAACGTCACAC
RANKL	Real time primers	239	AATTCCCCTGAAGGTACTCG	TCCTTTTTGGCTATGTCAGC
TNF-α	Real time primers	201	CCCACTCTGACCCCTTTACT	TTTGAGTCCTTGATGGTGGT
TGF-β	Real time primers	162	GCTACCATGCCAACTTCTGT	CGTAGTAGACGATGGGCAGT
IL-1 β	Real time primers	180	CCCAACTGGTACATCAGCAC	TCTGCTCATTCACGAAAAGG
IL-6	Real time primers	187	CTACCCCAATTTCCAATGCT	ACCACAGTGAGGAATGTCCA
IL-10	Real time primers	250	AGTGGAGCAGGTGAAGAGTG	TTCGGAGAGAGGTACAAACG
CD73	Real time primers	179 156	AGTCCAACCTCTCGCCTACT TCTGCAGCAAGTCAT TACCA	ATGACTCACCAAAGGCACAT CAGGTCTCCAGAGGCAGATA
CD39	Real time primers	166 228	TCTTAAACACCCTTCCACCA AGACAGACGAGGGAAGAGGA	TGGTGCCTAATTGTCTCCAT CAGGTTGGTGTGAGATGACC
Alpl	Real time primers	245 158	TCTGCTCAGGATGAGACTCC ACGAATCTCAGGGTACACCA	TCCCTTTTAACCAACACCAA TGAGCTTTTGGAGTTTCAGG
Runx2	Real time primers	154	CCACCTTCATTTGAATCCTG	GTTGGAGGCACACATAGGTC

Statistical analyses:

Simple univariate descriptive statistics in proportions, mean, median standard deviation and Standard error, where appropriate, was used to describe the dependent and independent variables of interest. Statistical significance between two groups was calculated using Student's t-test. Data from multiple-group experiments was analyzed by one-way ANOVA and post-hoc Tukey honestly significant difference (HSD). Bonferroni correction was used to adjust for possible Type-1 errors resulting from multiple comparisons. A p-value less than 0.05 was considered statistically significant.

Results:

I. *In-vitro* investigation to explain the role of nucleotides in RANKL mediated osteoclastogenesis:

1. *The effects of ADO and ADO receptor agonist (NECA) on RANKL induced osteoclastogenesis (Number of TRAP+ cells):*

In order to measure the mature osteoclasts differentiated from RAW264.7 cells when stimulated with RANKL (50 ng/ml) in the presence or absence of the 3 different ADO receptors agonists used in the experiment, differentiated osteoclasts were identified as TRAP+ multinuclear cells (cells containing more than 3 nuclei were counted).

A concentration of 1 or 10 nM of all 3 ADO receptor agonists used did not significantly affect the number of TRAP+ cells. However, a statistically significant higher number of TRAP+ cells were observed when concentrations of 100 and 1000 nM of both IB-MECA and CCPA were added. In contrast, concentrations of 100 and 1000 nM of NECA significantly lowered the number of TRAP+ cells. ***(Figure 1)***

2. *The effects of ADO and ADO receptor agonist (NECA) on RANKL induced osteoclastogenesis (pit formation assay):*

In order to evaluate the effect of NECA on the function of mature osteoclast cells, we performed pit formation assays using RANKL-stimulated RAW 264.7 as the source of mature osteoclasts. RAW 264.7 precursor cells that were stimulated with RANKL (50 ng/ml) and 3 different concentrations of NECA (10, 100, and 1000 nM) were added to Corning® Osteo Assay Surface (calcium phosphate-coated culture dishes to mimic the bone environment). The area of resorption on the plate surface was calculated.

The negative control group not stimulated with 50 ng/ml rRANKL showed no pit formation, as expected. Moreover, when the cells were treated with 10 nM of NECA, no difference was observed, confirming the results from the prior TRAP+ experiment. On the other hand, a significant decrease in osteoclastic activity occurred when cells were treated with 100 and 1000 nM of NECA by showing a smaller area of resorbed pits. ***(Figures 2 & 3)***

3. *The effects of ADO and ADO receptor agonist (NECA) on RANKL production by activated T-cells*

RANKL ELISA assay was performed on the culture supernatant of primary mouse T-cell cultures stimulated with anti-βTCR MAb and anti-CD28 MAb in the presence or absence of NECA (1, 10, 100 and 1000 nM). All 4 concentrations of NECA significantly suppressed the production of RANKL, showing downregulation of osteoclastogenesis and inhibition of osteoclastic activity. ***(Figure 4)***

3-H-thymidine radioisotope was added to the plates after collecting the culture supernatant. The plates were incubated in optimal conditions (37°C and 5% CO_2) for 24 hours. A concentration of 1 nM NECA had no effect on the proliferation of T lymphocytes; however, all other concentrations (10, 100, and 1000 nM) significantly downregulated the proliferation of T lymphocytes. ***(Figure 5)***

II. ATP kinetics in mouse periradicular lesions:

In order to monitor the kinetics of eATP, isolated samples were prepared for the bioluminescence assay for quantitative detection of ATP. The plate luminescence was measured after a 15-minute incubation period using the Synergy™ HT Multi-Mode Microplate Reader. A statistically significant difference was noted between wild-type (WT) mice and $CD73^{-/-}$Foxp3-$GFP^{+/+}$ mice at all 3 time points (7, 14, and 21 days). More specifically, an increase of ~10% in ATP expression levels was seen in KO mice when compared to WT mice at day 7. The difference was higher on day 14 with an increase of ~15%. Finally, on day 21, samples showed an increase in ATP production by ~20% in KO mice compared to WT. ***(Figure 6)***.

III. ADO loss of function effects on mouse periradicular lesion:

1. The effect of CD73 gene knockout on pulp exposure induced bone resorption

- H&E staining: ***(Figures 7 & 8)***

In order to evaluate the effect of ADO on proinflammatory status and the development of periradicular lesions, histomorphological paraffin sections of periradicular lesion (day 0, 7, 14, and 21) of both $CD73^{-/-}$Foxp3-$GFP^{+/+}$ and WT mice were evaluated and compared.

Histomorphological analysis of nonexposed teeth (day 0) served as a control to show the baseline of the periradicular area, periodontal ligament, and nature of inflammatory cells around the tooth apex.

An expansion and destruction of the periodontal ligament was observed in the periradicular area. This expansion significantly increased on days 7, 14, and 21. This

destruction was more evident in CD73$^{-/-}$Foxp3-GFP$^{+/+}$ mice. At days 14 and 21, diffuse inflammatory cell infiltration could be observed. Particularly, infiltration of PMNs was clearly noted in the CD73-/-Foxp3-GFP+/+ group when compared to WT. This suggests that the absence of ADO and accumulation of ATP in the periradicular area could upregulate the mediation of proinflammatory cytokines and attract inflammatory cells. Periradicular bone destruction was also significantly greater at all time points in the CD73$^{-/-}$Foxp3-GFP$^{+/+}$ mice.

- TRAP staining: ***(Figures 9, 10 & 11)***

There was significantly higher number of TRAP+ cells were observed in the periradicular area of CD73$^{-/-}$Foxp3-GFP$^{+/+}$ mice in all time points.

- Immunofluorescence staining: ***(Figure 12)***

Immunofluorescence staining of periradicular lesion of day 21 WT mice with 3 antibody staining: DRAQ5 for nucleus, FITC for Foxp3+, and Alexa Flour 594 for CD73. Yellow areas seen in the confocal microcopy images are double positive stained with FITC and Alexa Flour 594 confirming that Foxp+ T_{reg} cells express CD73.

- µCT analysis: ***(Figures 13 & 14)***

Periradicular lesions were initiated by pulp exposure of the mandibular first molar pulp of 8-week-old C57BL/6J mice or CD73$^{-/-}$Foxp3-GFP$^{+/+}$ mice (C57BL/6J background) at 4 different time points: 0, 7, 14, and 21 days (n=10/group). Mandibular jaws were collected from mice sacrificed at respective time points (0, 7, 14 and 21 days) and hemisectioned. The right side of the hemisectioned mandible was defleshed, rinsed

with PBS and fixed in 4% paraformaldehyde solution overnight. After extensive washing under running water for 1 to 3 hours, the fixed jaw was subjected to micro-computed tomography (μCT) using compact fan-beam-type tomograph (μCT40, Scanco Medical AG, Basserdorf, Switzerland) at the Forsyth microCT core facility following Balto et al. [67].

The size of the periradicular lesions in $CD73^{-/-}$Foxp3-$GFP^{+/+}$ mice significantly increased at days 7, 14, and 21. More specifically, the size of periradicular lesions increased in $CD73^{-/-}$Foxp3-$GFP^{+/+}$ mice when compared to WT mice in groups sacrificed at days 7, 14, and 21 by 0.084, 0.072, and 0.184 mm^2, respectively.

2. *Detection of mRNA expression for CD39, CD73, proinflammatory, anti-inflammatory cytokines, osteoclast and osteoblast differentiation markers.*

In order to assess the effect of CD73 gene knockout (loss-of-function) on the inflammatory process in periradicular lesions, left hemimandibles were isolated from euthanized WT and $CD73^{-/-}$Foxp3-$GFP^{+/+}$ mice at days 0, 7, 14 and 21 (n=10/group). The bone block was trimmed to include only the root apices of the first molars after decoronation of the coronal part of the tooth. mRNA extraction was performed, as shown in Material and Methods. Gene expression of CD73, CD39, IL-1β, IL-6, TNF-α, TGF-β, RANKL, OPG, ALP, and RUNX2 mRNA was evaluated by qPCR using β-actin as an internal control.

a) CD73 and CD39:

The expression of CD73 in WT mice showed significant increase on days 14 and 21 in a time-dependent manner, suggesting host defense against the inflammatory

process ***(Figure 15)***. Meanwhile, the expression of CD39 in WT mice showed a trend of gene overexpression in a time-dependent manner, even though statistically significant increase was only observed on day 21. When CD39 expression was evaluated in CD73$^{-/-}$Foxp3-GFP$^{+/+}$ mice, results showed an increase in gene expression in a time-dependent manner with statistically significant difference seen on days 14 and 21. When data from both WT and CD73$^{-/-}$Foxp3-GFP$^{+/+}$ mice were compared, CD39 expression was slightly higher in CD73$^{-/-}$Foxp3-GFP$^{+/+}$ with no statistically significant difference ***(Figure 16)***. In general, these findings indicate that the immune system is trying to prevent ATP accumulation in periradicular lesions by upregulating CD73 and CD39 with the objective of increasing the production of ADO.

b) Proinflammatory mediators:

The expression pattern of IL-1β mRNA in the periradicular lesions of WT and CD73$^{-/-}$Foxp3-GFP$^{+/+}$ mice showed statistically significant increase at all three time points (7, 14, 21 days) when compared to the nonexposed control samples. However, when WT and CD73$^{-/-}$Foxp3-GFP$^{+/+}$ mice were compared to each other, statistically significant difference was only observed on day 14 and 21 ***(Figure 17)***.

A time-dependent pattern of IL-6 gene expression was displayed in the periradicular lesions of WT and CD73$^{-/-}$Foxp3-GFP$^{+/+}$ mice; however, this increase was only statistically significant on day 21. When evaluating the difference between WT and CD73$^{-/-}$Foxp3-GFP$^{+/+}$ mice, a huge increase of IL-6 expression was noted in KO mice, especially on days 14 and 21 ***(Figure 18)***.

The expression of TNF-α mRNA in the periradicular lesions of WT mice showed a spike on day 7. Following this, expression dropped on day 14, but increased on day 21. On the other hand, the expression levels in CD73$^{-/-}$Foxp3-GFP$^{+/+}$ mice were higher at all-time points and reached a plateau at day 14. Most importantly, a noticeably higher expression of TNF-α was observed in CD73$^{-/-}$Foxp3-GFP$^{+/+}$ mice, especially on days 14 and 21 ***(Figure 19)***.

Generally, these findings underscore the importance of CD73 and ADO in minimizing the overexpression of proinflammatory cytokines in periradicular lesions.

c) Anti-inflammatory mediators:

The expression pattern of TGF-β mRNA in the periradicular lesions of WT and CD73$^{-/-}$Foxp3-GFP$^{+/+}$ mice showed significant increase at the 14- and 21-day time points when compared to nonexposed control samples. However, no difference was detected between WT and CD73$^{-/-}$Foxp3-GFP$^{+/+}$ mice ***(Figure 20)***.

d) Osteoclast differentiation factors:

Although no difference in OPG mRNA expression was detected between WT and CD73$^{-/-}$Foxp3-GFP$^{+/+}$ mice ***(Figure 21)***, upregulation of RANKL showed statistically significant difference in CD73$^{-/-}$Foxp3-GFP$^{+/+}$ mice ***(Figure 22)***.

e) Osteoblast differentiation factors:

A time-dependent pattern of gene expression of RUNX2 mRNA was displayed in the periradicular lesions of WT mice; however, this increase was only statistically significant on day 14. On the other hand, the expression of RUNX2 in the periradicular

lesions of CD73$^{-/-}$Foxp3-GFP$^{+/+}$ mice showed no change at day 7 compared to the nonexposed control group. RUNX2 expression then spiked on day 14. Following this, a slight drop in expression was detected at day 21. Notably, no significant difference in RUNX2 production was observed between WT and CD73$^{-/-}$Foxp3-GFP$^{+/+}$ mice ***(Figure 23)***.

A time-dependent increase in gene expression pattern of alkaline phosphatase (ALP) was displayed in the periradicular lesions of WT mice; however, this increase was not statistically significant. Meanwhile, the expression of ALP in the periradicular lesions of CD73$^{-/-}$Foxp3-GFP$^{+/+}$ mice showed no change on day 7 compared to the nonexposed control group. However, ALP expression spiked at day 14. Following this, a slight drop in expression was detected at day 21. Notably, no significant difference in ALP production was seen between WT and CD73$^{-/-}$Foxp3-GFP$^{+/+}$ mice ***(Figure 24)***.

IV. ADO gain of function effects on mouse periradicular lesion:

1. The effect of NECA administration on pulp exposure induced bone resorption:

A total of 15 black wild-type (WT) mice (C57BL/6J) were used in this experiment (8 weeks; body weight 25-30 g). Mice were anesthetized by intraperitoneal injection of Ketamine HCl (80 mg/kg of body weight) and Xylazine (10 mg/kg) in sterile phosphate-buffered saline (PBS). Periradicular lesions were initiated by pulp exposure of the mandibular first molar pulp. On the day of pulp exposure, NECA at 0.1mg/kg/day was systemically administered i.p. (n=5/group). The other group received i.p. injections with the same volume of PBS (n=5/group) to standardize the stress levels induced during

injections and minimize any confounding factors. Finally, the last five mice without pulp exposure were used as negative control (n=5/group). All mice were sacrificed on day 21, and samples were immediately collected. Mandibular jaws were collected from the mice sacrificed for morphologic, histologic and molecular evaluation. The mandible was hemisected, and the left side mandibular jaw was immediately frozen at −70°C for RNA extraction. The right side was defleshed, rinsed with PBS and fixed in 4% paraformaldehyde solution overnight. After extensive washing under running water for 1 to 3 hours, the fixed jaw was subjected to micro-computed tomography (μCT) prior to decalcification and histological evaluation.

The fixed jaw was subjected to micro-computed tomography (μCT) using a compact fan-beam-type tomograph (μCT40, Scanco Medical AG, Basserdorf, Switzerland) at the Forsyth microCT core facility following Balto et al. [67]. The μCT results showed a significant decrease in the size of the periradicular lesions when NECA was administered. The difference in the size of periradicular lesions was statistically significant with ~2.5-fold decrease. ***(Figures 25 & 26)***

2. *Detection of mRNA expression for pro-inflammatory, anti-inflammatory cytokines, CD39, CD73, and CD73 receptors in periradicular lesions:*

In order to evaluate the effect of NECA administration (gain-of-function) on the inflammatory process in periradicular lesions, left side hemimandibles were isolated from euthanized mice at day 21 (n=5/group). The bone block was trimmed to include only the root apices of the first molars after decoronation of the coronal part of the tooth. mRNA extraction was performed as shown in material and methods. Gene expression

of CD73, CD39, IL-1β, IL-6, TNF-α, TGF-β, RANKL, ALP, and RUNX2 mRNA was evaluated by qPCR using β-actin as an internal control.

a) CD73 and CD39: ***(Figures 27 & 28)***

The expression of CD73 mRNA and CD39 mRNA in NECA-treated mice showed significant increase *(P<0.01)* suggesting host defense against the inflammatory process. Generally, these findings highlight the prevention of ATP accumulation in the periradicular lesions by upregulating CD73 and CD39 to allow for increased production of ADO.

b) Proinflammatory mediators: ***(Figures 29, 30 & 31)***

The expression of mRNAs for IL-1β, IL-6, and TNF-α in the periradicular lesions of NECA-treated mice showed downregulated gene expression. However, statistical significance was only detected in IL-1β gene expression *(P<0.01)*. These data underscore the importance of ADO in modulating host response and preventing the influx of proinflammatory mediators to the periradicular area.

c) Anti-inflammatory mediators: ***(Figure 32)***

The expression of TGF-β mRNA in the periradicular lesions of NECA-treated mice showed the same levels of gene expression when compared to nontreated mice.

d) Osteoclast differentiation factors: ***(Figure 33)***

The expression levels of RANKL mRNA in periradicular lesions of NECA-treated mice were significantly lower *(P<0.01)*. These data highlight the critical role of ADO in

downregulating the expression of this gene encoding osteoclast differentiation factor, RANKL.

e) Osteoblast differentiation factors: ***(Figures 34 & 35)***

The expression of RUNX2 mRNA in periradicular lesions of NECA-treated mice showed higher gene expression; however, this increase was not statistically significant. On the other hand, the expression of ALP in periradicular lesions of NECA-treated mice showed a significant increase by 3-fold when compared to nontreated mice.

Comparison between the effects of CD73 gene knock-out (loss of ADO function) and NECA-treated mice (gain of function):

	CD73-KO	NECA-treated
Proinflammatory cytokines		
IL-1β	(+)	(-)
IL-6	(+)	NS
TNF-α	(+)	NS
Anti-inflammatory cytokines		
TGF-β	NS	NS
Osteoblast differentiation factors		
RUNX2	NS	NS
ALP	NS	(+)
Osteoclast differentiation factors		
RANKL	(+)	(-)
OPG	NS	NS
Ectoenzymes		
CD73	Knocked-out	(+)
CD39	NS	(+)

(+) upregulated *(P < 0.05)*
(-) downregulated *(P < 0.05)*
(NS) No statistical significance detected

Discussion:

Despite increased understanding on the effects of bacteria-derived PAMPs on the etiology of periradicular periodontitis [68-72], the role of damage-associated molecular pattern molecules (DAMPs) that are released from host immune surveillance cells in the context of periradicular periodontitis is largely unknown. It is plausible that, in response to bacterial challenge, DAMPs released from damaged host cells are involved in the up-regulation of inflammation in the context of infection [73-76], the theory of which can be applied to the periradicular periodontitis. However, among a panel of DMAPs that are thus far reported to be released from damaged host cells, extracellularly released ATP, ADO, and other purine metabolites have relatively recently identified as DAMPs [77-80]. For this reason, the possible engagements of ATP and ADO in the inflammatory bone resorption processes in periradicular periodontitis have been largely unknown until this study. The present study, for the first time, addressed and established the pathophysiological roles of ATP and ADO in the context of periradicular periodontitis.

In this study, we have investigated the roles of purine family DAMPs, ATP and ADO, and CD73 ectonucleotidase, the enzyme that catalytically converts ATP-metabolite AMP to ADO in the pathogenically dysregulated bone remodeling processes of periradicular periodontitis using a mouse model. $CD73^{-/-}$Foxp3-$GFP^{+/+}$ mice showed significantly elevated inflammatory response after the induction of periradicular periodontitis compared to that induced in wild-type mice (Figures 17, 18 & 19). Also, the number of TRAP+ multinucleated osteoclastic cells in the periradicular area as well as the size of bone loss was significantly larger in the CD73-KO mice than those detected

in WT mice (Figures 11 & 14), suggesting that CD73 is engaged in the suppression of osteoclast-mediated bone resorption. Furthermore, CD73 expression was predominantly found on Foxp3+ T_{reg} cells, but not on the other cell types, in the mouse periradicular lesion (Figure 12). All of above noted findings supported our hypothesis that extracellular adenosine (eADO) produced by CD73+Foxp3+ T_{reg} cells may play a counter-regulatory role in bone resorption induced in periradicular periodontitis.

The role of purine nucleotides in induction of inflammatory response in periradicular periodontitis:

The pathogenic bone resorption occurring in periradicular periodontitis is a multifactorial process. Pro-inflammatory cytokines and immune cells are critical players in this task [81-86]. However, besides bacterial PAMPs, the upstream molecular events that elicit the production of inflammatory factors and activate immune cells are largely unknown. While consensus support that bacterial PAMPs trigger the inflammatory immune responses in most cases of periradicular periodontitis [68-70], it is also true that, even after the successful disinfection of root canal system by virtue of root canal antibacterial procedure, inflammation and bone resorption process in the periradicular periodontitis are retained [87-89], suggesting the presence of endogenous factor(s) that can activate the inflammatory immune responses in addition to latent bacterial infection. For this reason, we explored pathophysiological effects of purine metabolites as most abundant DAMPs that are released by host cells in response to bacterial infection.

In this study, it was demonstrated that the CD73 expressed on Treg cells can convert proinflammatory ATP to anti-inflammatory ADO that, in turn, suppressed RANKL-mediated osteoclastogenesis and RANKL production by activated T-cells (Figure 22). CD39/CD73 adenosinergic machinery changes dynamically the property of proinflammatory ATP [90, 91]. More specifically, CD39 exonucleases convert proinflammatory ATP to AMP which is, in turn, transformed to anti-inflammatory ADO by means of CD73's nuclease activity [43, 91]. Most importantly, Foxp3+ Treg cells co-express CD39 and CD73 [63, 90], while both CD39 and CD73 are also reported to be expressed by endothelial cells [92, 93]. It is becoming increasingly recognized that altering this CD39/CD73 machinery can change the course several pathophysiological events, such as AIDS, autoimmune diseases, infections, atherosclerosis, ischemia-reperfusion injury, and cancer [94-102]. In this regard, recent studies revealed that T_{regs} cells are the major cellular source for CD73 and CD39 ectonucleotidases in inflammatory immune responses [41, 42]. Although the possible engagement of CD39/CD73 adenosinergic exonucleases expressed on Treg cells have been largely unknown, the present study demonstrated that the CD73 expressed on Treg cells can convert proinflammatory ATP to anti-inflammatory ADO that, in turn, suppressed RANKL-mediated osteoclastogenesis and RANKL production by activated T-cells.

The effects of ADO and ADO receptor agonist (NECA) on RANKL induced osteoclastogenesis

A recent study showed that CD73 produced by T_{regs} down-regulated the production of NF-κB through the activation of adenosine receptor A_{2A} and reducing the

production of proinflammatory mediators [44]. Another study highlighted the importance of ADO and its receptors in the pathophysiology of bone metabolism and inflammatory bone resorption, opening “new areas for exploration in understanding endogenous control of bone metabolism” [103]. All of the previous reports clearly concur to our results showing that increased level of ADO via CD73 may lead to the inhibition of the RANKL-mediated osteoclastogenesis and downregulation of the inflammatory bone resorption.

The effects of ADO and ADO receptor agonist on RANKL production by activated T-cells

Accumulated lines of evidence support that activated T cells express RANKL in the context of periradicular inflammatory bone resorption and the level of RANKL production was also directly related to the expansion of periradicular bone loss lesion [24, 33, 104]. Several pharmacological agents that suppress the RANKL-induced osteoclastogenesis, such as, a cathepsin K inhibitor odanacatib (ODN) [105], alendronate [106] and ATP6i-silencing shRNA [107], were demonstrated to suppress periradicular bone loss induced in animal models. However, since all of those approaches that target only osteoclasts without regulating the production of RANKL by activated T cells, it is concerned if those approaches would cause side effects similar to MRONJ [108]. Therefore, additional investigations are required prior to the translation of those findings into the treatment of human periradicular periodontitis. On the other hand, growing evidence emphasizes that ADO receptor agonists especially that target A_{2a} receptor may lead to the development of modalities that can suppress pathogenic

inflammatory immune responses [109, 110]. It was reported that A_{2a} receptor plays an immune-suppressive roles [111], which involve ADO-mediated Treg activation [112, 113] as well as direct suppression of effector T cells [114]. However, no studies have addressed the effect of ADO and its receptors on RANKL production by activated T cells. Our results showed that ADO receptor agonist (NECA) significantly suppressed the production of RANKL from activated T cells and down-modulated the RANKL-induced osteoclastogenesis as well as osteoclastic pit-formation activity *in vitro* (Figures 2 & 4), suggesting that the approach to activate ADO receptors can suppress the pathogenic bone resorption in the periradicular periodontitis by acting on activated T cells that produce RANKL. Very importantly, we did not observe any sign of osteonecrosis in the mice induced of periapical periodontitis that received systemic administration of NECA (data not shown).

ATP kinetics in mouse periradicular lesions:

ATP is one of the most intensively studied molecules in the classical biology. Based on ATP's intracellular roles to store and transfer energy, ATP is known as the "energy currency" of cells [115]. However, surprisingly, ATP and other purine nucleotides can be released into the extracellular spaces by cell lysis or by non-lytic mechanisms under certain conditions [43, 116]. Indeed, the proinflammatory effect of extracellular ATP was uncovered by the discovery of ATP receptors expressed on cell surface, such as P2X and P2Y [117, 118]. More specifically, ATP elicits a major endogenous danger signal via ligation to the purinergic receptors, leading to the production of proinflammatory cytokines from surrounding leukocytes, such as T cells

and macrophages that express ATP receptors [119-121]. High concentration of ATP in the extracellular spaces induce a predominantly proinflammatory effects [116]. Above noted earlier studies coincide with our finding that $CD73^{-/-}$Foxp3-$GFP^{+/+}$ mice showed an accumulation of ATP in the periradicular lesion in a time dependent manner (Figure 6), probably due to the absence of CD73-dependent catalytic action to convert ATP-metabolite AMP to ADO.

Adenosine loss of function model effects on periradicular bone resorption:

CD73 expression in wild-type periradicular periodontitis:

Although there was no studies looked at the presence and function of CD73 in the context of oral disease pathogenesis especially periradicular periodontitis, our results demonstrated a time dependent increase in the expression of CD73 gene in WT mice using qPCR. Moreover, frozen immunofluorescence histological stained sections showed clear expression of $CD73^{+}$ $Foxp3^{+}$ cells in the periradicular lesions.

The effect of CD73 gene knockout on pulp exposure induced bone resorption:

Previous reports showed that development of periradicular lesions in mouse models takes around 72 hours to show innate immune cells migration to the area and 3 days to show adaptive immune cells migration [12, 122, 123]. The peak of periradicular lesion size will reach at day 21 after the pulp exposure [124].

Our data showed that $CD73^{-/-}$Foxp3-$GFP^{+/+}$ had significantly higher amount of periradicular bone resorption compared to WT mice due to the accumulation of ATP in the extracellular spaces. Knockout mice also exhibited more intense inflammatory cells

infiltration into the periradicular lesions. Moreover, Knockout mice showed a higher number of TRAP+ cells in the periradicular area.

Reports in the literature indicated that higher levels of ATP in the tissues with diminished amounts of ADO may lead to exaggerated immune response and promoting mononuclear cells chemotaxis [43, 103]. Taken together, these findings firmly suggest the role of ADO and CD73 in the pathogenesis of periradicular periodontitis and subsequent supporting bone loss.

The effect of CD73 gene knockout on mRNA expression for CD39, proinflammatory, anti-inflammatory cytokines, osteoclast and osteoblast differentiation markers:

- CD39 (Ectonucleoside triphosphate diphosphohydrolase-1):

CD39 ectonucleotidase represents the first step in the metabolism of purine nucleotides which mainly dephosphorylates extracellular ATP to AMP. CD39 is crucial in the conversion of extracellular ATP and catalytic inactivation which is an important mechanism of immune suppression [125]. In our results, gene expression was slightly higher in $CD73^{-/-}$Foxp3-$GFP^{+/+}$ mice with no statistical significant difference in all time points.

- Proinflammatory mediators:

There is growing evidence in the literature that CD39 and CD73 expressed by T_{reg} cells contribute to local accumulation of adenosine, suppressing proinflammatory cytokine production, and attenuation of inflammation [91, 126]. Therefore, increasing the levels of ADO in the extracellular spaces will lead to reduction in proinflammatory cytokines generation.

Our results as expected match all the previously mentioned studies, showing overall increase in the proinflammatory cytokine production in $CD73^{-/-}$Foxp3-$GFP^{+/+}$ mice by virtue of decrease ADO levels.

- Anti-inflammatory mediators:

The literature shows that anti-inflammatory cytokines levels are directly proportional to the levels of CD39 and CD73. Moreover, TGF-β anti-inflammatory cytokine signaling directly induce the generation of these ectonucleotidases [127, 128]. In our data, although there was a significant increase of TGF-β in days 14 and 21 after the pulp exposure, however, there was no statistical difference between the wild-type and knockout mice.

- Osteoclast differentiation factors:

There is a consensus in the literature that extracellular ATP stimulates the expression RANKL. On the other hand, extracellular ADO will counteract the ATP actions and suppress the RANKL expression [103, 129-131]. Our data showed an immense increase in RANKL expression in $CD73^{-/-}$Foxp3-$GFP^{+/+}$ compared to wild-type mice. However, OPG expression didn't show a statistical difference between the two groups in all time points.

- Osteoblast differentiation factors:

There has been an increase interest in the literature to study and explore the potential role of ADO in osteoblast differentiation. Recently, studies showed that CD73 generated ADO regulate the differentiation of osteoblasts through A_{2B} receptor signaling [55, 132-134]. However, in our results RUNX2 and ALP didn't show a significant

difference between wild-type and knockout mice although there was a trend of increase in the expression of RUNX2 at day 21 in $CD73^{-/-}$Foxp3-$GFP^{+/+}$ mice.

Adenosine gain of function model effects on periradicular bone resorption:

The effect of NECA administration on pulp exposure induced bone resorption:

There was no real interest in the effects of ATP and adenosine in oral inflammatory diseases even though these molecules have an important role in pain perception and signaling too which is vital element in dental research [131]. Given the high number of agonists and antagonists for these molecules, our focus was to develop a novel therapeutic regimen for human periradicular periodontitis.

In order to choose the best possible agent to modulate the immune response and minimize the bone resorption, 3 different adenosine receptor agonists were tested *in vitro* as explained above. NECA exhibited a significant reduction in the osteoclastic activity validating testing it in an *in vitro* model to confirm its action.

The mice received intraperitoneal systemic administration of non-selective adenosine receptor agonist NECA started at the day of pulp exposure by 0.1mg/kg/day, i.p. as shown in the materials and methods section. These mice showed diminished amount of periradicular bone resorption confirming the previous *in vitro* results and opening the door for more thorough investigation in this area. Moreover, these mice showed a statistical significant decrease in the expression of CD39, CD73, IL-1β, and RANKL. Additionally, there was a huge increase in alkaline phosphatase expression showing the higher osteoblast activity in NECA treated mice.

Similarly, the literature showed that A_{2B} AR knockout mice exhibited a reduction in osteoblast differentiation factors (ALP and RUNX2) [132]. Also, the overall proinflammatory and anti-inflammatory effects of NECA reported were very similar to our data. Taken together, NECA has the potential to be a key pharmacological element used in local immune modulation for therapeutic purposes.

Conclusions:

1) According to *in vitro* assays, adenosine receptor agonist, NECA, significantly suppressed not only RANKL-mediated osteoclastogenesis from RAW264.7 cells, but also significantly downregulated proliferation and RANKL production from TCR/CD28-activated T cells, suggesting that the ADO elicited signal can downregulate RANKL-induced osteoclastogenesis.
2) As determined by qPCR-based *in vivo* gene expression analysis, the amount of ATP and expression of CD73 mRNA were significantly increased in the mouse periradicular lesion in a time-dependent manner, indicating that CD73 expression may be induced to down-regulate the inflammation that is elicited by elevated ATP.
3) Systemic administration of NECA to the mice induced of periradicular periodontitis significantly upregulated the mRNA expressions for CD39, CD73, alkaline phosphatase, and RUNX2, while downregulated the expressions of mRNAs for RANKL and IL1-β, accompanied by diminished size of periradicular lesion, compared to the control no-drug-treated WT mice that were induced of periradicular periodontitis. These results implicated that activation of ADO receptor-signaling can not only suppress the osteoclast-mediated bone resorption, but also promote the osteoblastogenic-bone formation.

4) Fluorescent immunohistochemical staining of mouse periradicular lesion showed that CD73 was prominently expressed by Foxp3+ T_{reg} cells infiltrating in the lesion, while modest level of CD73 expression was detected in endothelial cells, suggesting Treg cells are the major cellular source of CD73 in the periradicular lesion.
5) Finally, the locally produced ATP and mRNAs for RANKL, IL1-β, IL-6, and TNF-α, as well as the size of periradicular lesions were significantly larger *(P<0.05)* in $CD73^{-/-}$ Foxp3-$GFP^{+/+}$ mice compared to control WT-mice, as periradicular periodontitis was induced in those two different mouse strains, supported the role of Foxp3+ T_{reg} cells in converting ATP to ADO which, in turn, facilitates the anti-inflammatory effects in the context of periradicular periodontitis.

Table of Figures:

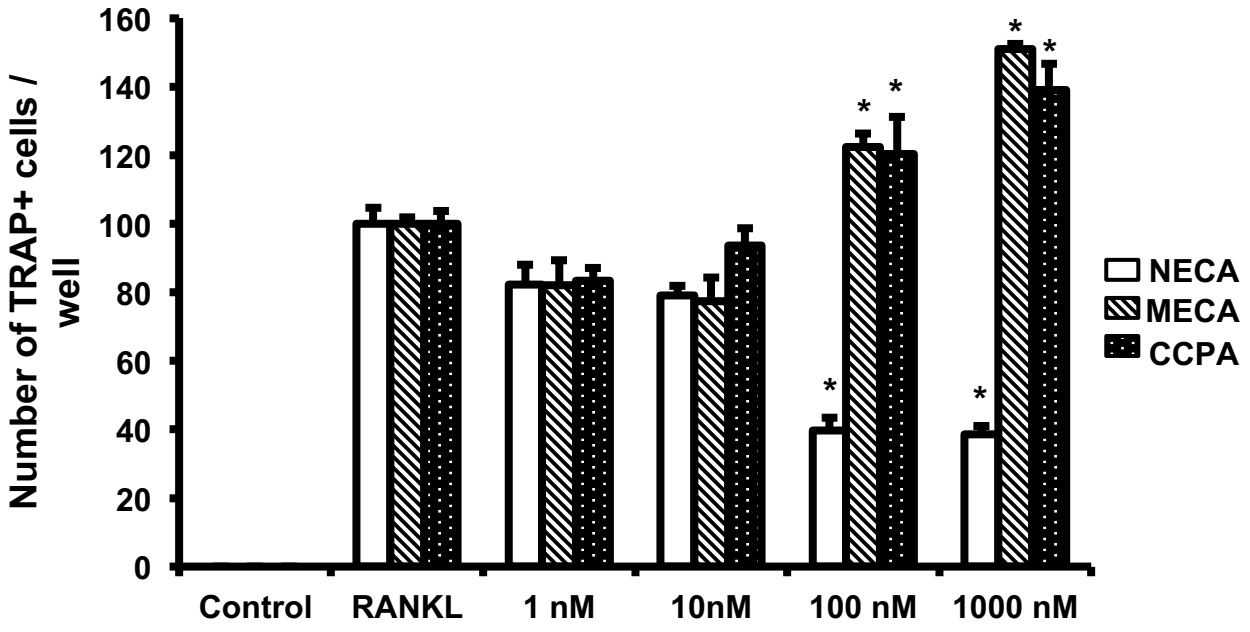

Figure 1. Number of TRAP+ mature osteoclasts differentiated from RAW264.7 cells when stimulated with RANKL (50 ng/ml) in the presence or absence of 4 different concentrations of 3 different ADO receptors agonists.

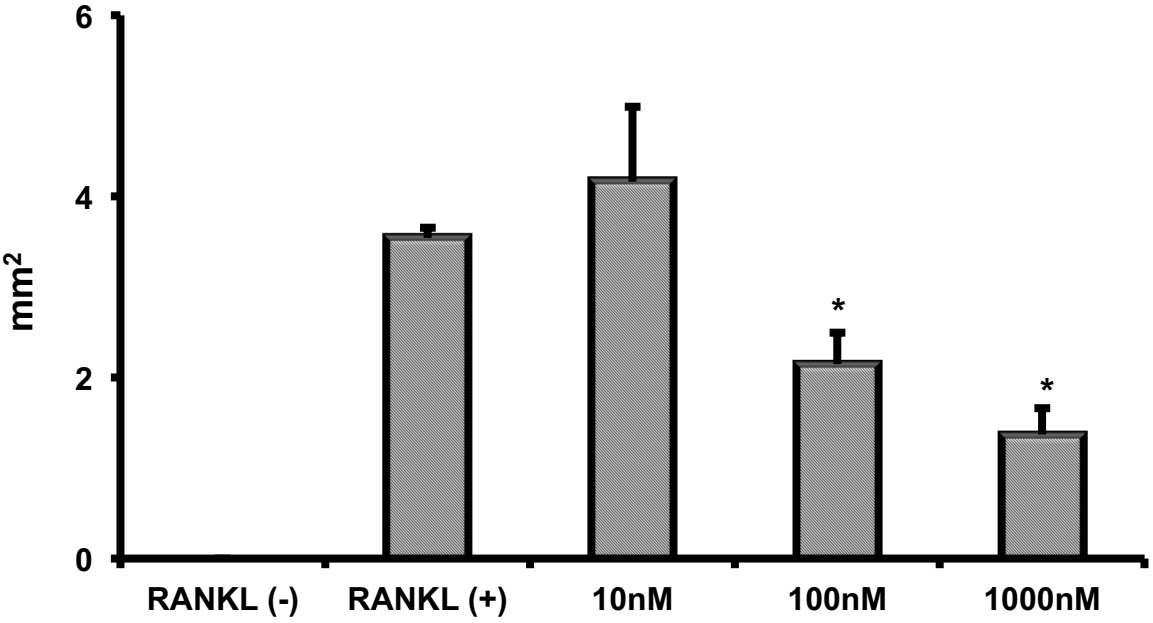

Figure 2. Effect of ADO receptor agonist (NECA) on RANKL induced Osteoclastogenesis by pit formation assay. **(P < 0.05).*

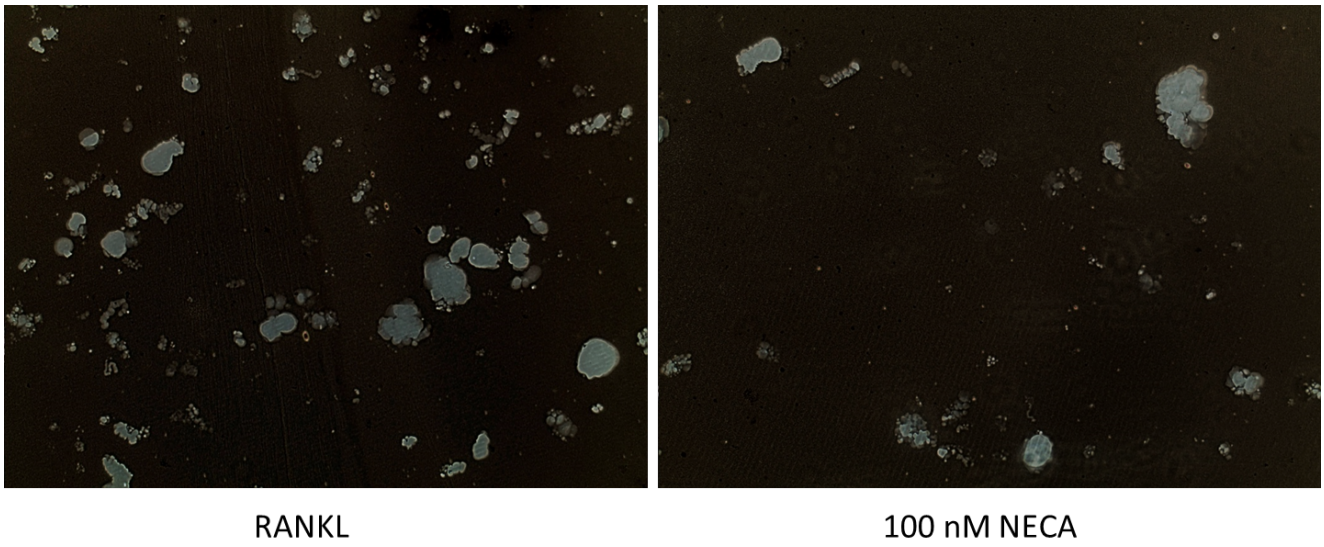

Figure 3. Photomicrographs of resobed areas in the osteo assay plate by mature osteoclasts in 2 different groups. (x40)

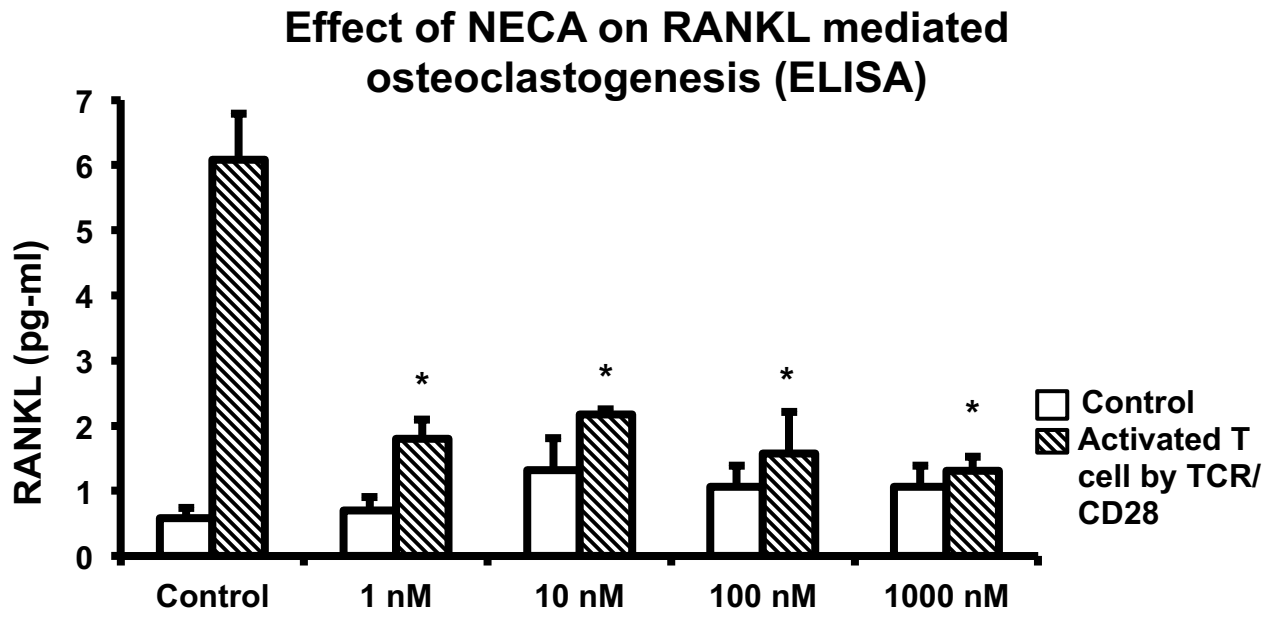

Figure 4. ELISA assay was performed on the culture supernatant of primary mouse T-cell cultures that were stimulated with anti-βTCR MAb and anti-CD28 MAb in the presence or absence of NECA

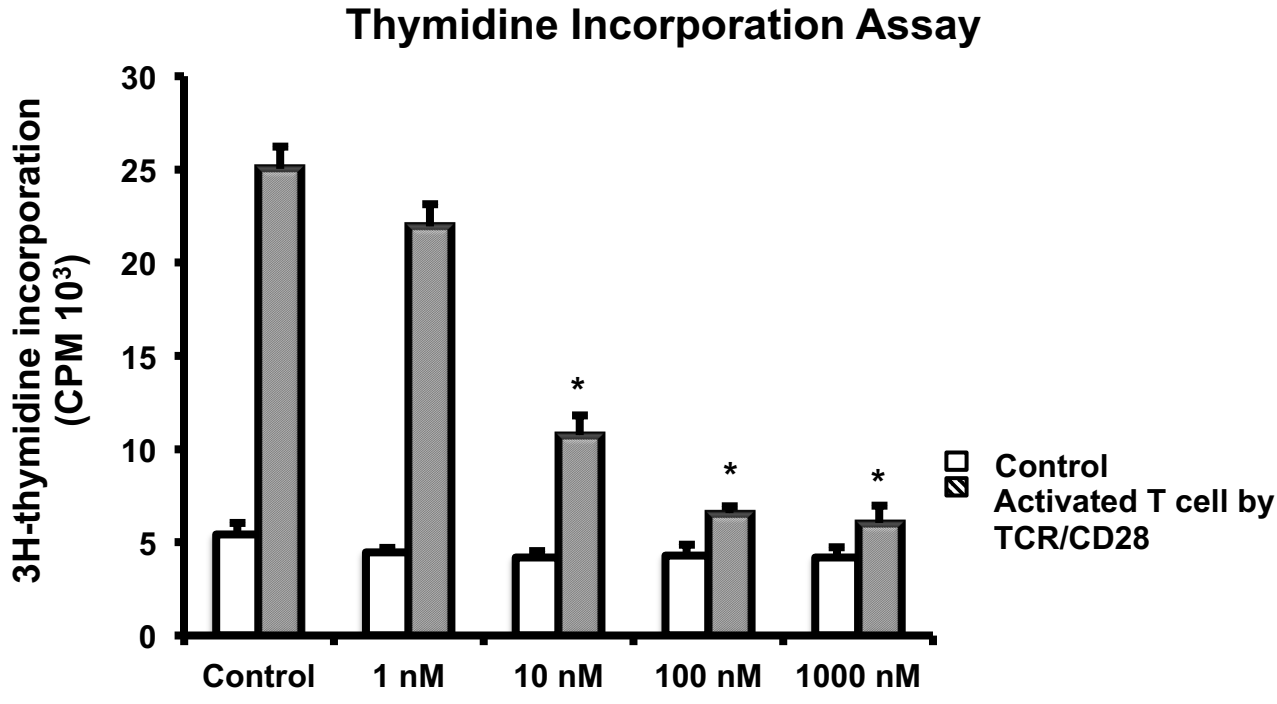

Figure 5. 3-H-thymidine radioisotope incorporation assay. **(P < 0.05).*

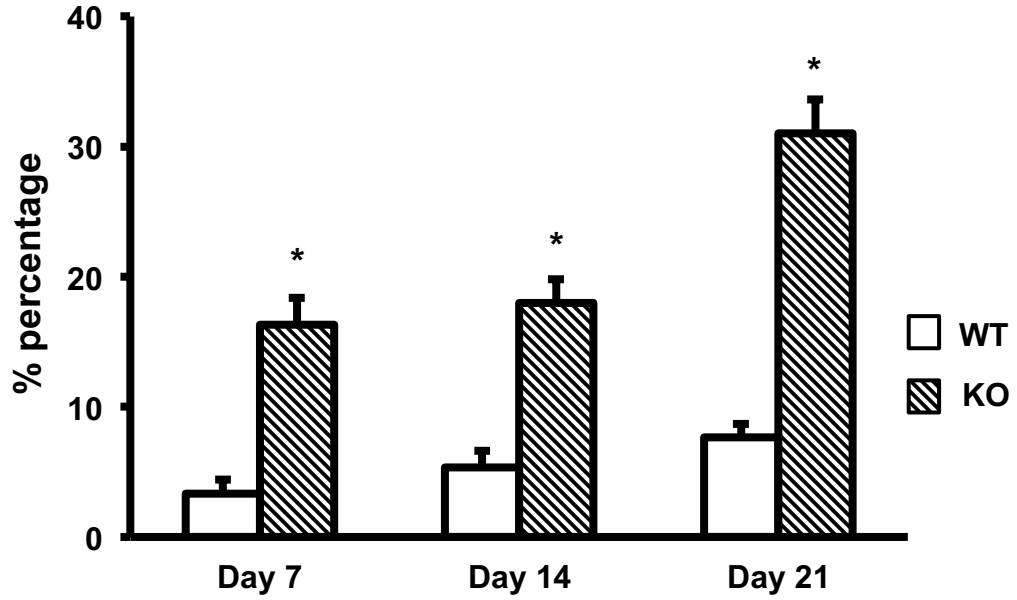

Figure 6. Percentage difference of ATP levels detected in the Periradicular lesions of WT and KO mice at different time points post pulp exposure. *$(n = 7, P < 0.05)$.

A)

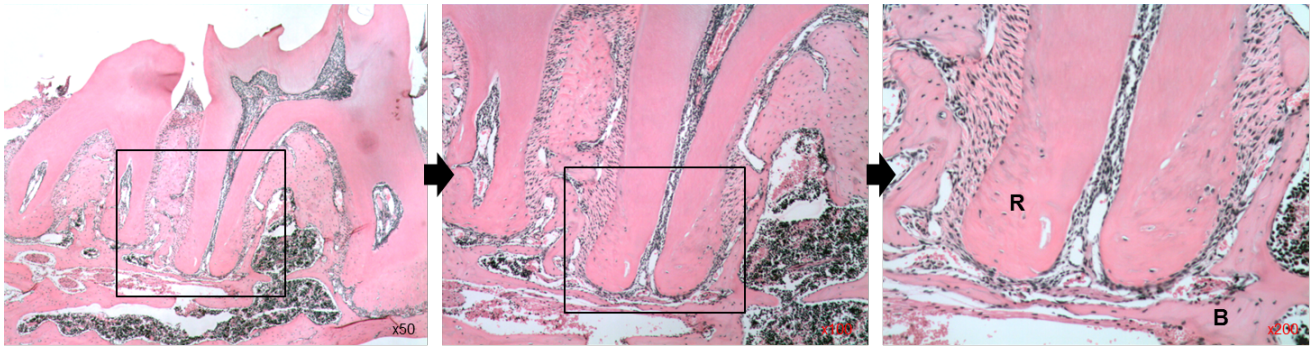

B)

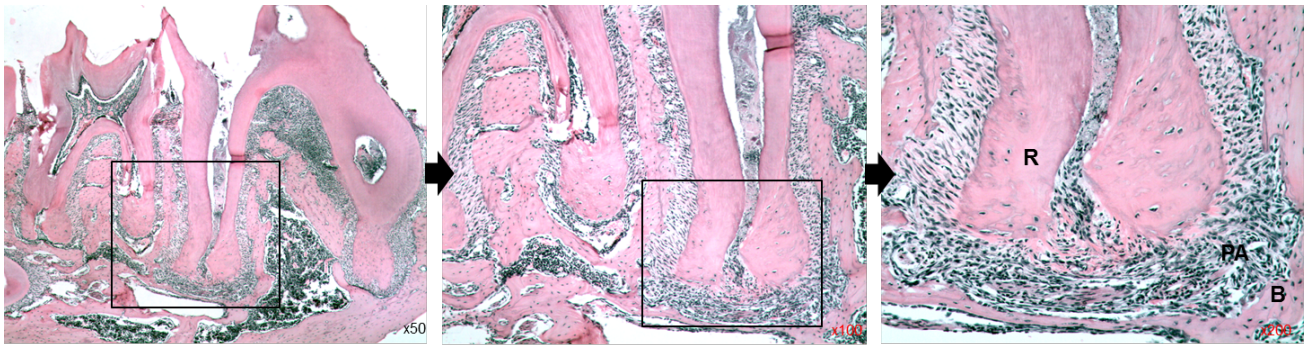

Figure 7. **A)** photomicrographs of histological sections stained with H&E staining of the WT control (non-exposed) mice. **B)** WT 21 days following pulp exposure. **R:** Root; **PA:** Periradicular lesion; **B:** Bone

A)

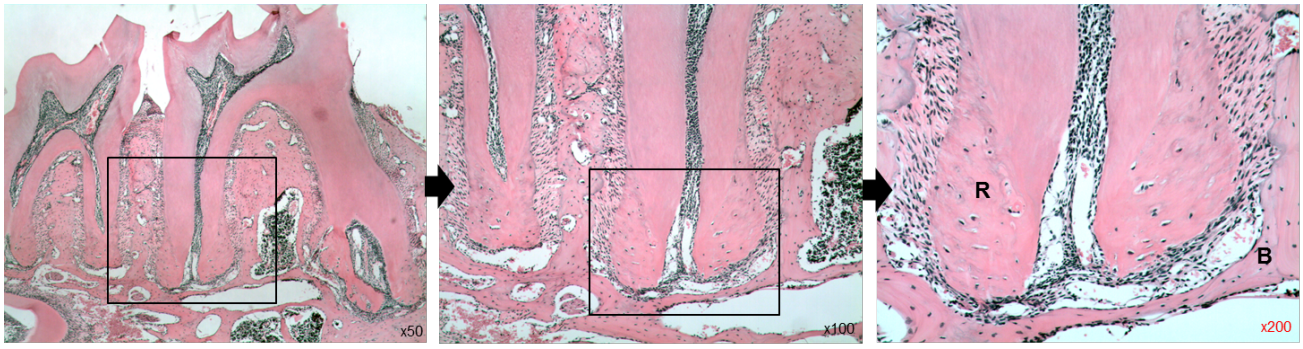

B)

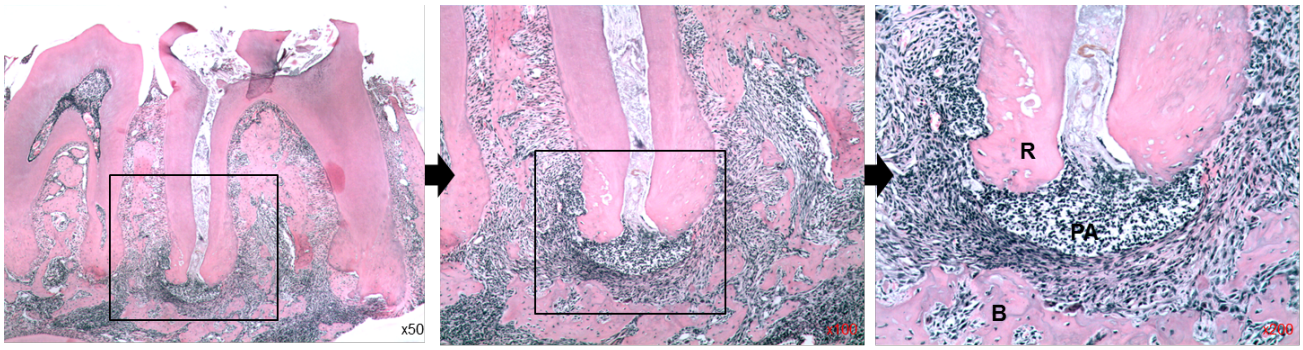

Figure 8. **A)** photomicrographs of histological sections stained with H&E staining of the KO control (non-exposed) mice. **B)** KO 21 days following pulp exposure. **R:** Root; **PA:** Periradicular lesion; **B:** Bone

A)

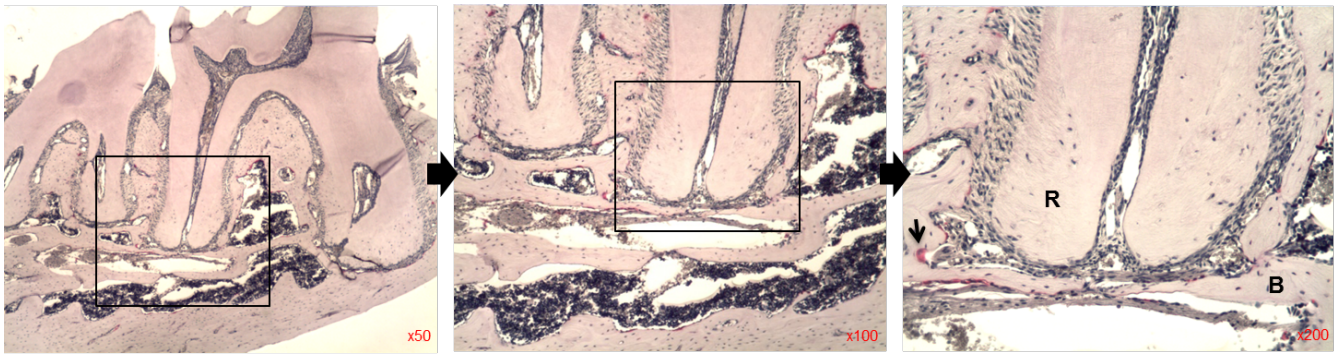

B)

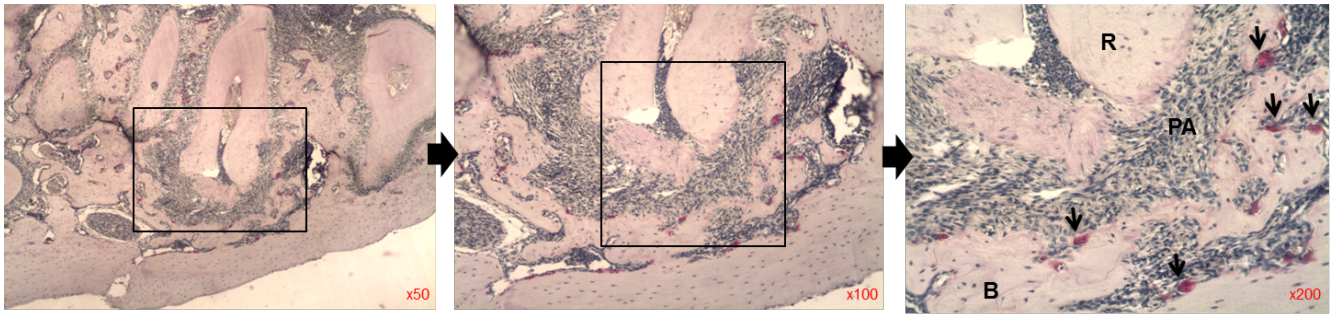

Figure 9. **A)** photomicrographs of histological sections stained with TRAP staining and counter satined with hematoxylin of the WT control (non-exposed) mice. **B)** WT 21 days following pulp exposure. **R:** Root; **PA:** Periradicular lesion; **B:** Bone; arrows indicate the TRAP+ osteoclasts in the lesion.

A)

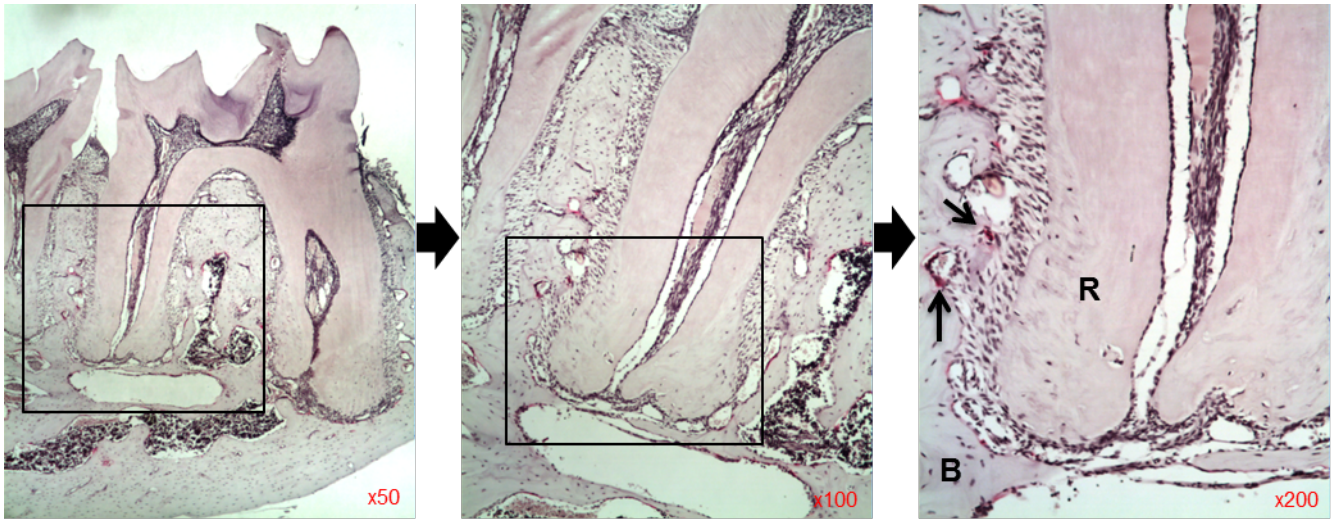

B)

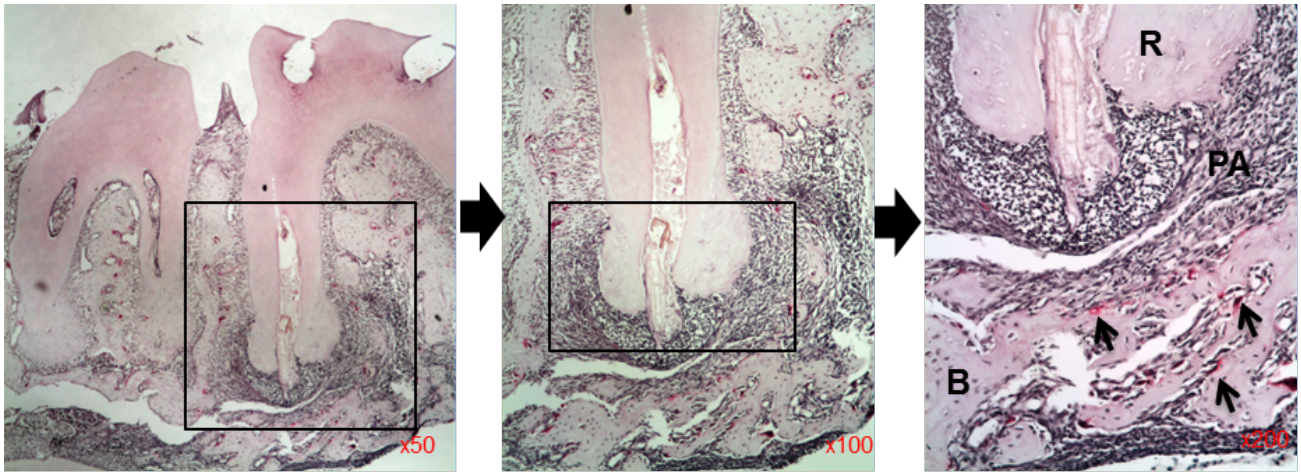

Figure 10. **A)** photomicrographs of histological sections stained with TRAP staining and counter satined with hematoxylin of the KO control (non-exposed) mice. **B)** KO 21 days following pulp exposure. **R:** Root; **PA:** Periradicular lesion; **B:** Bone; arrows indicate the TRAP+ osteoclasts in the lesion.

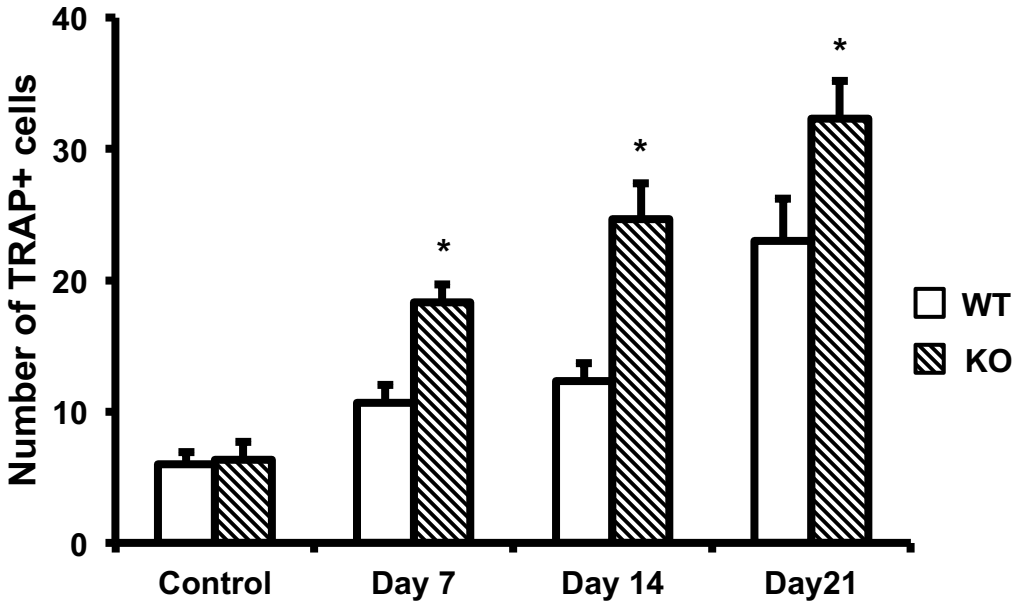

Figure 11. Number of TRAP+ cells in WT and KO mice at different time points.

**(n = 5, P < 0.05).*

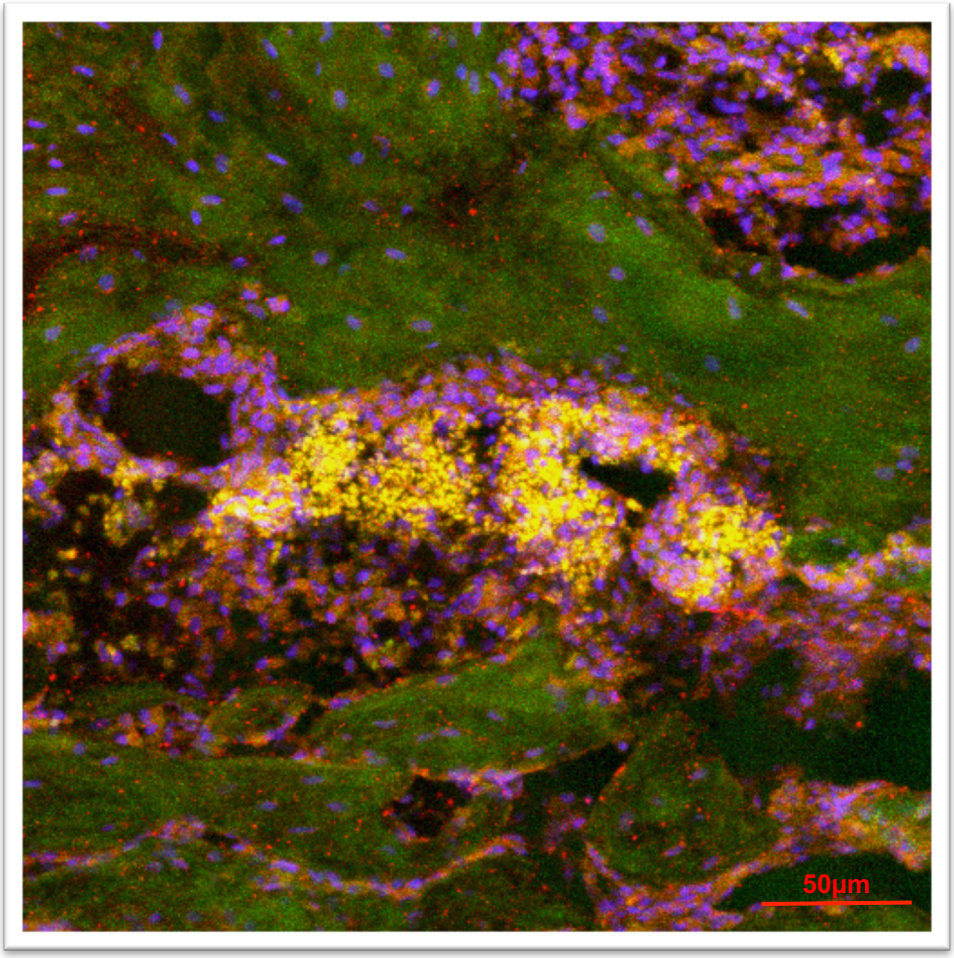

Figure 12. Immunofluorescence staining of periradicular lesion of day 21 WT mice (Blue: nucleus with DRAQ5, Green: Foxp3 with FITC, Red: CD73 with Alexa Flour 594). Yellow areas are double-positive cells stained with FITC and Alexa Flour 594. Green area represents the bone.

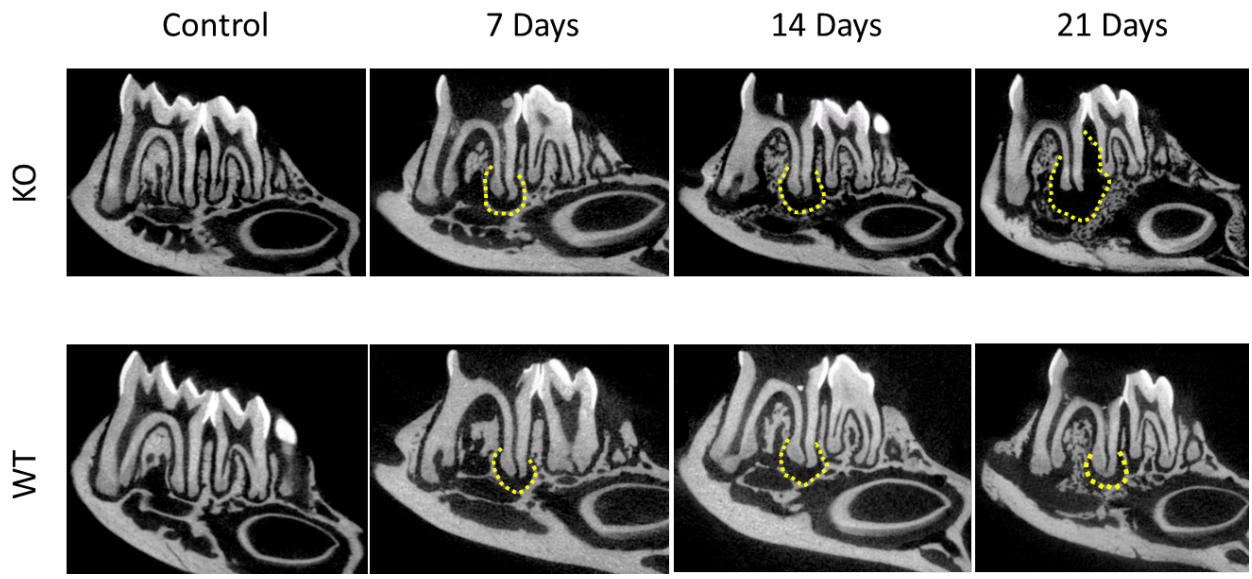

Figure13. Buccal view slice showing the amount of bone resorption

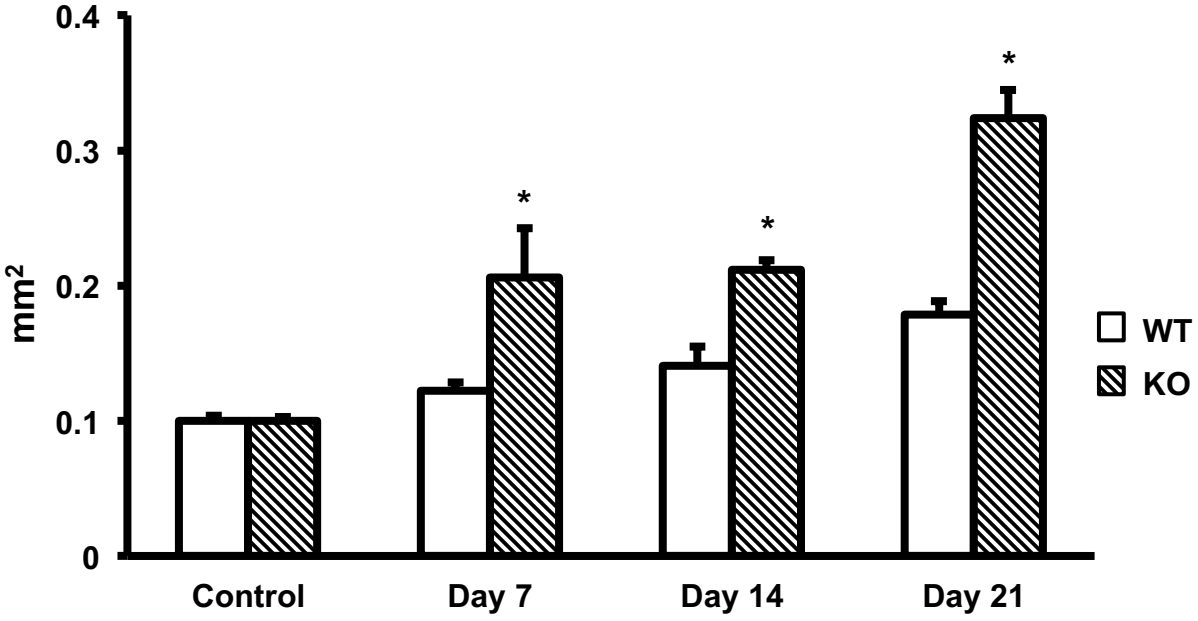

Figure 14. Quantification of bone resorption by μCT analysis

**(n = 10, P < 0.05).*

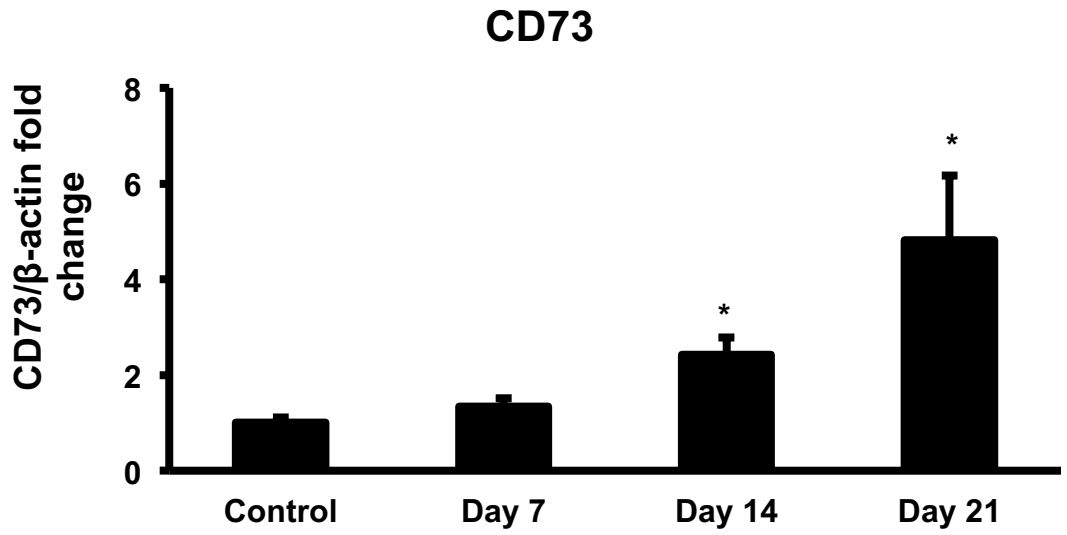

Figure 15. CD73 mRNA expression in WT Periradicular lesions showing CD73 gene expression fold change relative to beta actin housekeeping gene in multiple time points. **(n = 10, P < 0.05).*

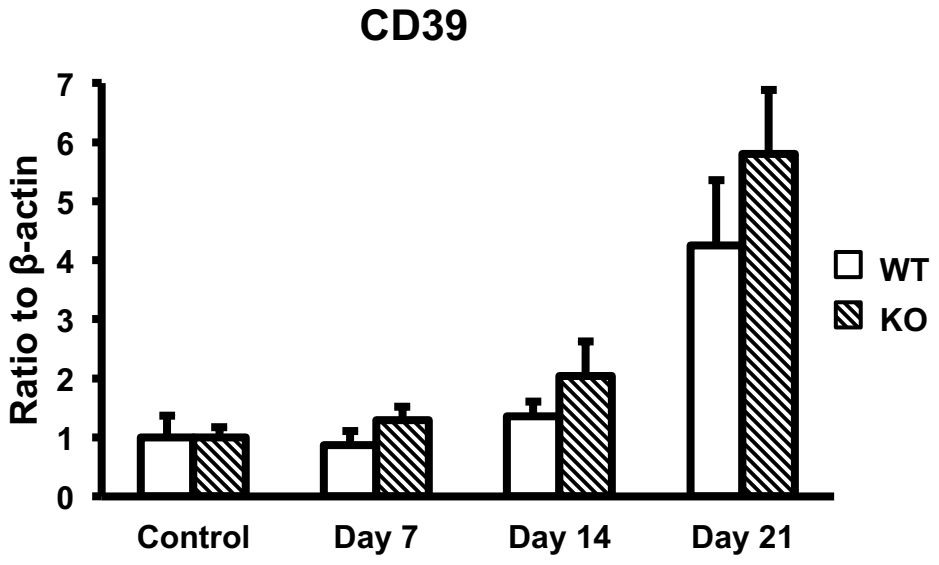

Figure 16. CD39 mRNA expression in WT and KO Periradicular lesions showing CD39 gene expression fold change relative to beta actin housekeeping gene in multiple time points. **(n = 10, P < 0.05).*

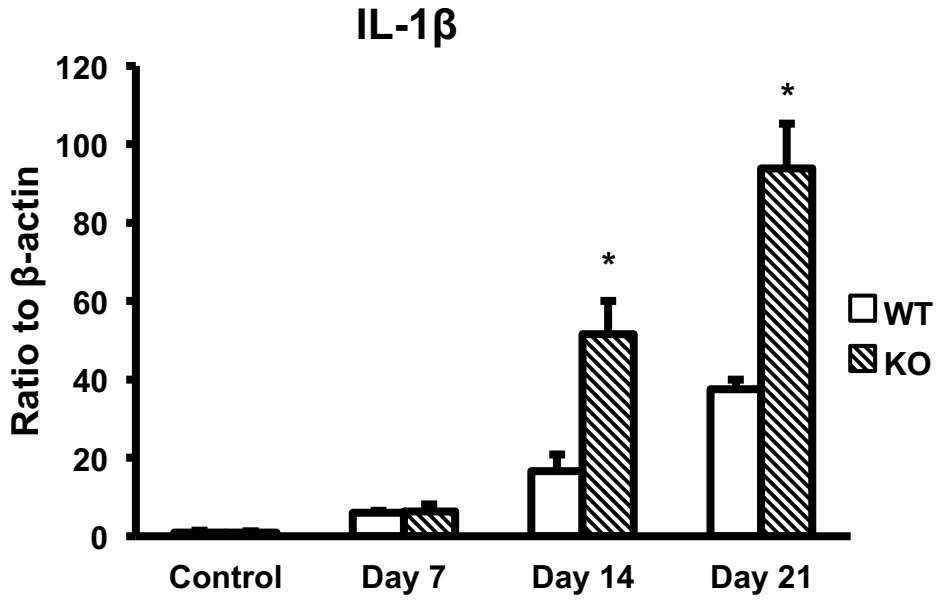

Figure 17. IL-1β mRNA expression in WT and KO Periradicular lesions showing IL-1β gene expression fold change relative to beta actin housekeeping gene in multiple time points. **(n = 10, P < 0.05).*

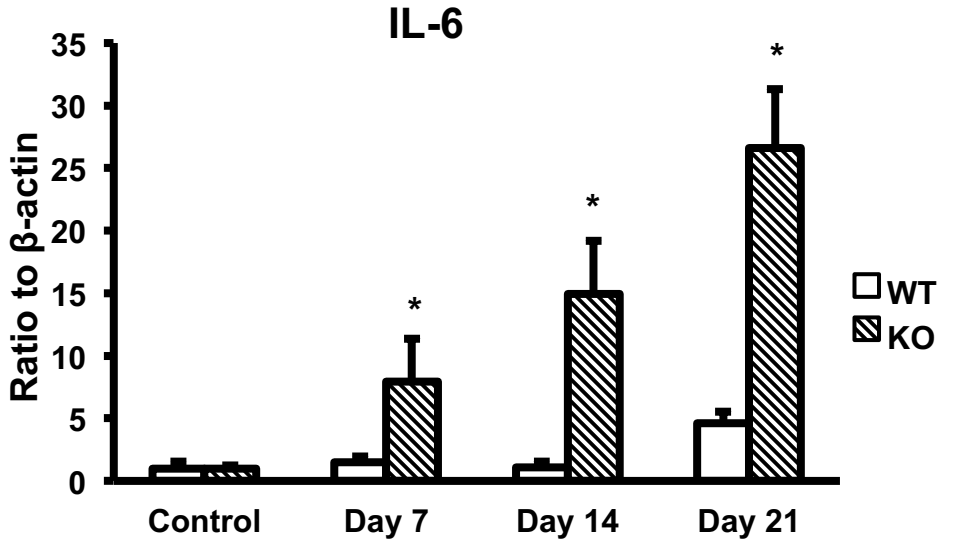

Figure 18. IL-6 mRNA expression in WT and KO Periradicular lesions showing IL-6 gene expression fold change relative to beta actin housekeeping gene in multiple time points. **(n = 10, P < 0.05).*

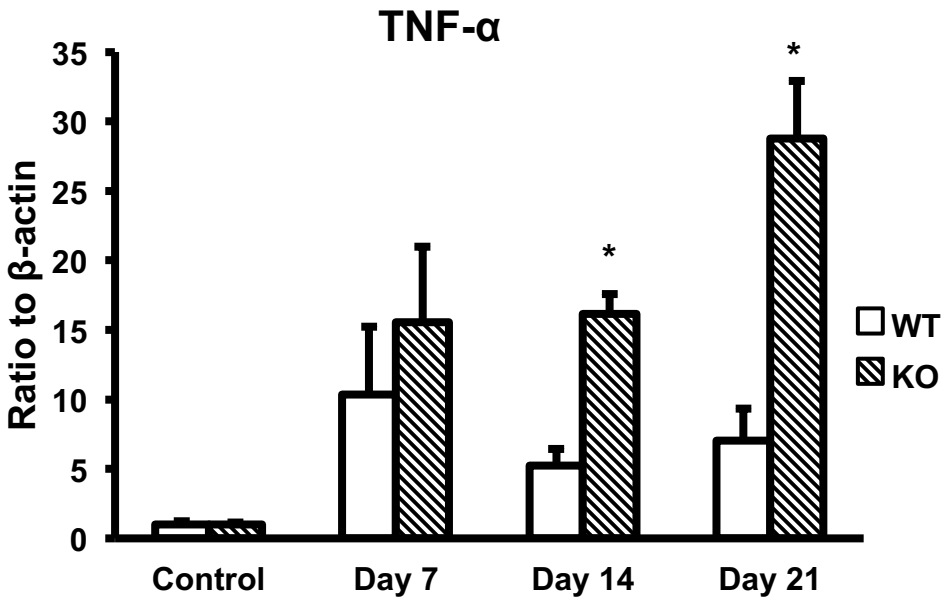

Figure 19. TNF-α mRNA expression in WT and KO Periradicular lesions showing TNF-α gene expression fold change relative to beta actin housekeeping gene in multiple time points. **(n = 10, P < 0.05).*

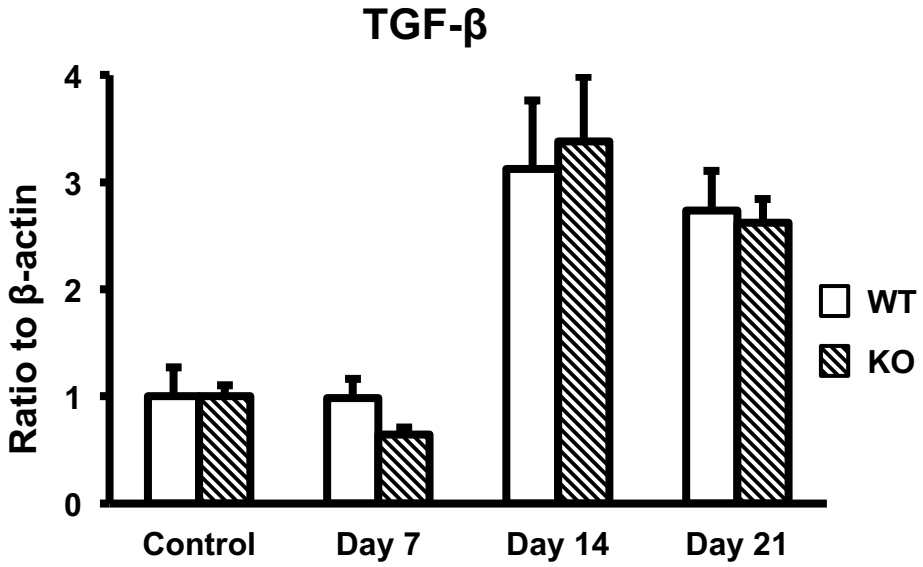

Figure 20. TGF-β mRNA expression in WT and KO Periradicular lesions showing TGF-β gene expression fold change relative to beta actin housekeeping gene in multiple time points. **(n = 10, P < 0.05).*

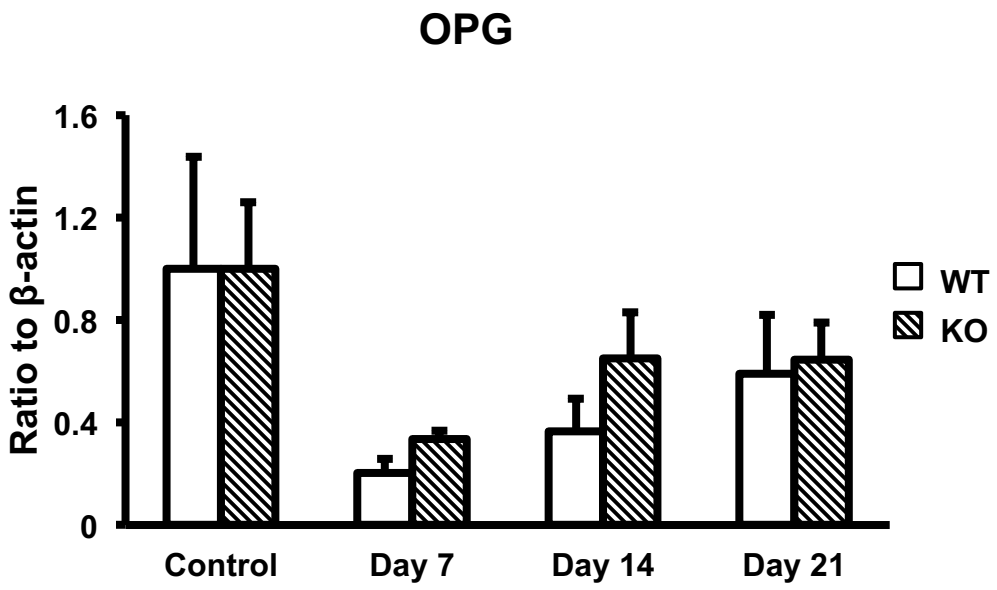

Figure 21. OPG mRNA expression in WT and KO Periradicular lesions showing OPG gene expression fold change relative to beta actin housekeeping gene in multiple time points. **(n = 10, P < 0.05).*

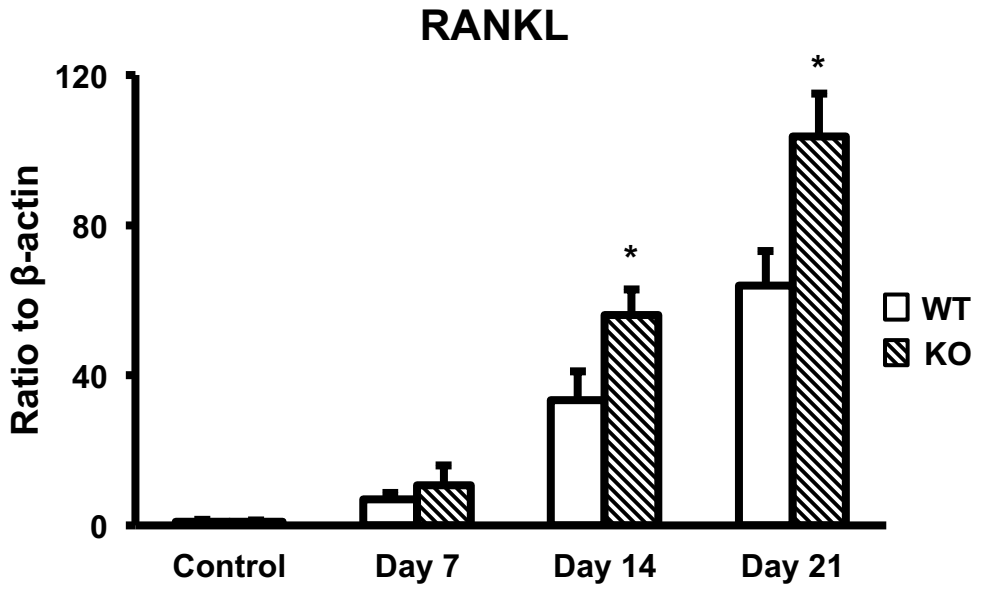

Figure 22. RANKL mRNA expression in WT and KO Periradicular lesions showing RANKL gene expression fold change relative to beta actin housekeeping gene in multiple time points. **(n = 10, P < 0.05).*

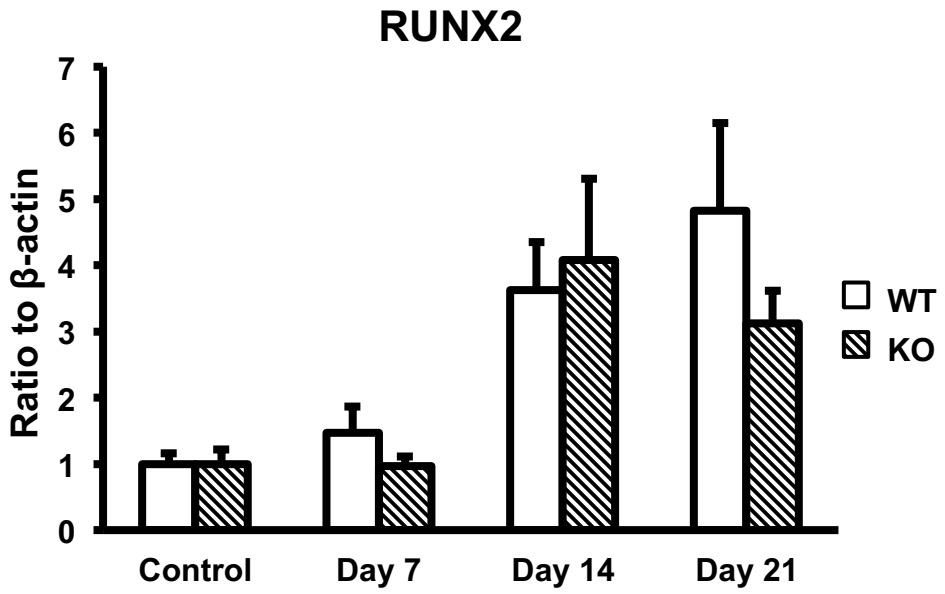

Figure 23. RUNX2 mRNA expression in WT and KO Periradicular lesions showing RUNX2 gene expression fold change relative to beta actin housekeeping gene in multiple time points. **(n = 10, P < 0.05).*

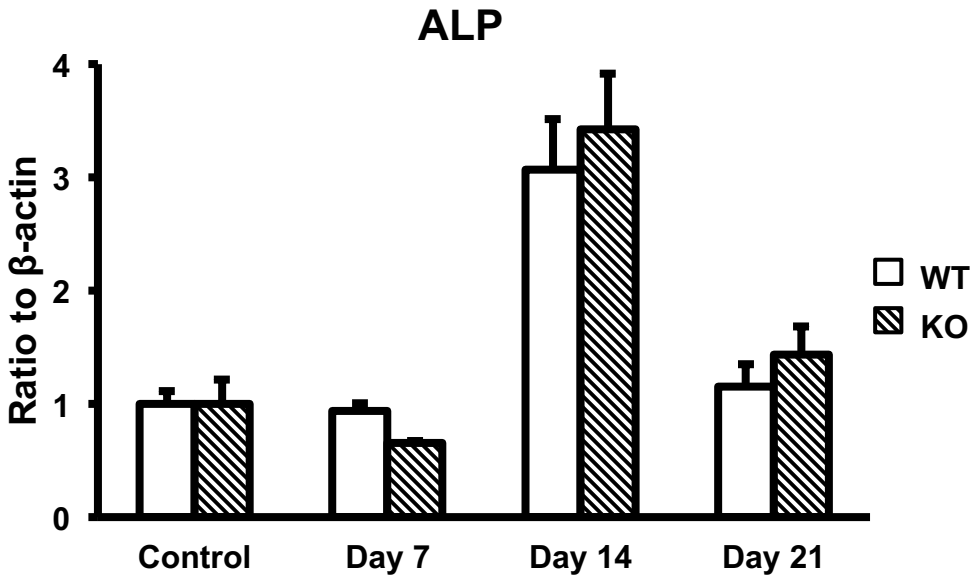

Figure 24. Alkaline phosphatase (ALP) mRNA expression in WT and KO Periradicular lesions showing ALP gene expression fold change relative to beta actin housekeeping gene in multiple time points. **(n = 10, P < 0.05).*

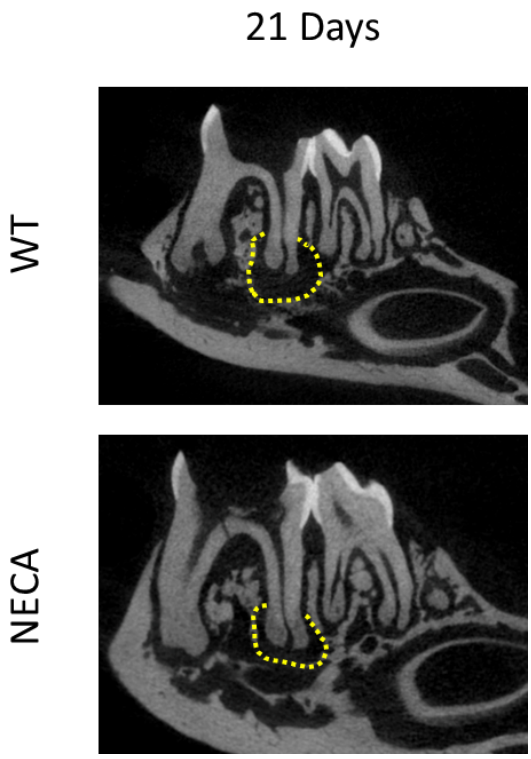

Figure 25. Buccal view slice showing the amount of bone resorption

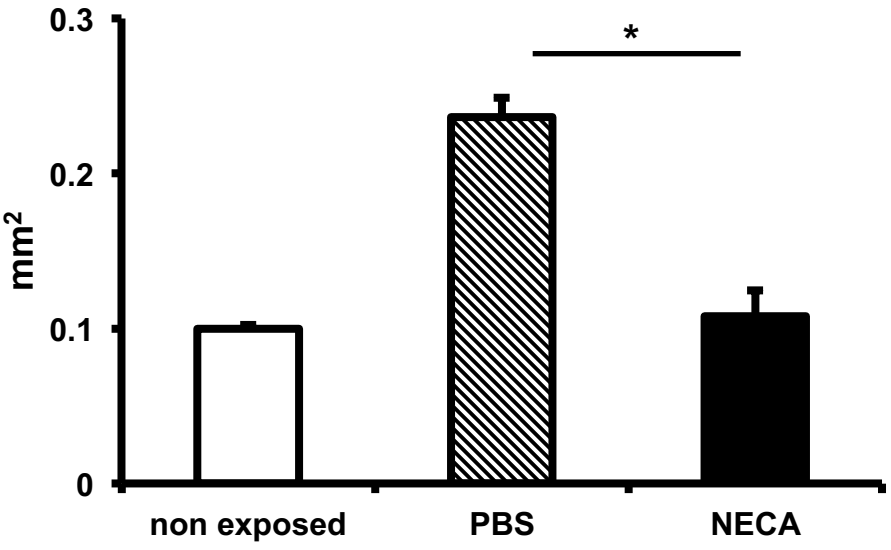

Figure 26. Quantification of bone resorption by µCT analysis

**(n = 5, P < 0.05).*

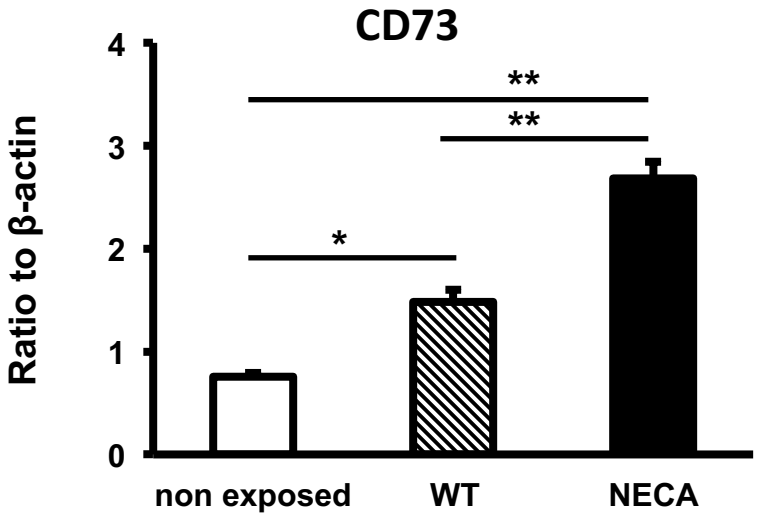

Figure 27. CD73 mRNA expression in WT non-exposed, WT PBS-treated and NECA-treated mice periradicular lesions showing CD73 gene expression fold change relative to beta actin housekeeping gene. *(n = 10, *P < 0.05 / **P < 0.01).*

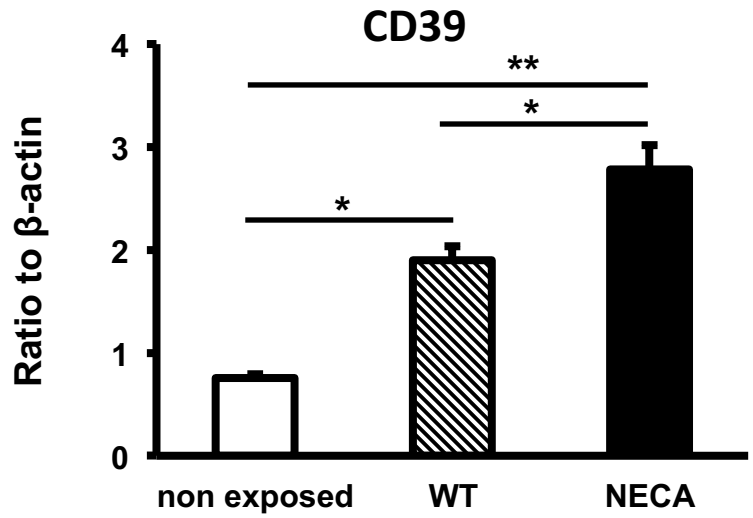

Figure 28. CD39 mRNA expression in WT non-exposed, WT PBS-treated and NECA-treated mice periradicular lesions showing CD39 gene expression fold change relative to beta actin housekeeping gene. *(n = 10, *P < 0.05 / **P < 0.01).*

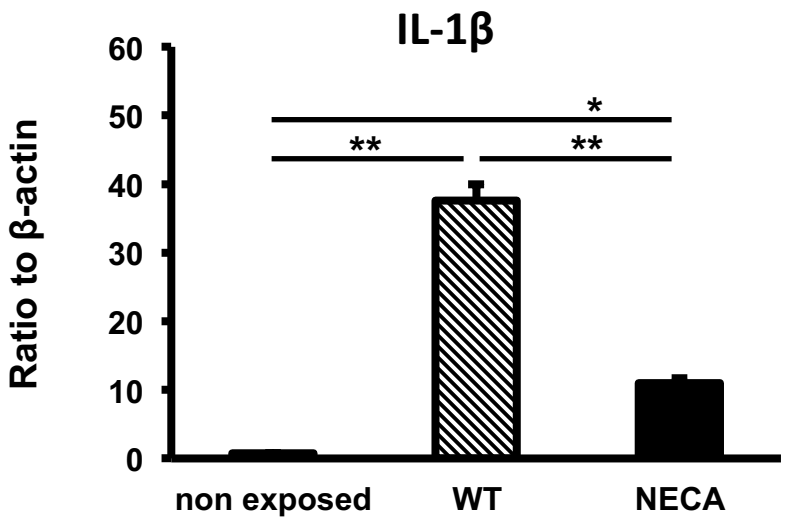

Figure 29. IL-1β mRNA expression in WT non-exposed, WT PBS-treated and NECA-treated mice periradicular lesions showing IL-1β gene expression fold change relative to beta actin housekeeping gene. *(n = 10, *P < 0.05 / **P < 0.01).*

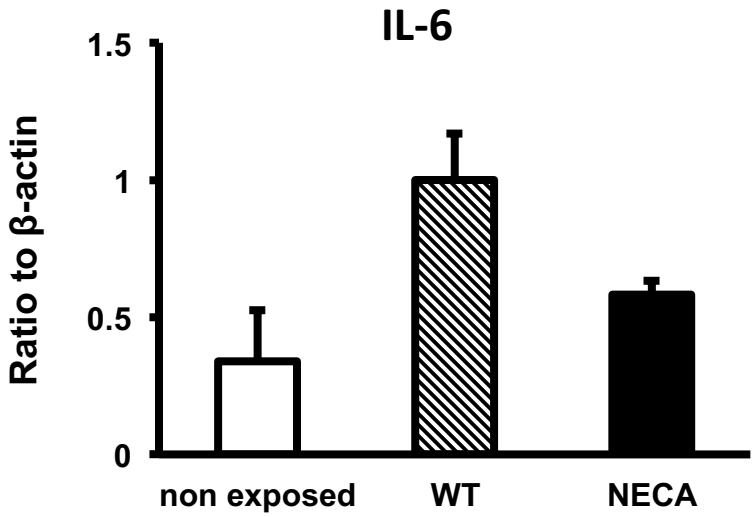

Figure 30. IL-6 mRNA expression in WT non-exposed, WT PBS-treated and NECA-treated mice periradicular lesions showing IL-6 gene expression fold change relative to beta actin housekeeping gene. *(n = 10).*

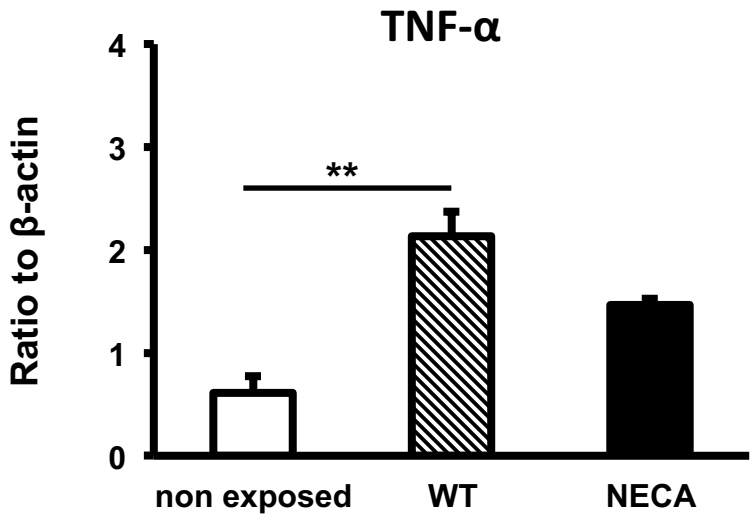

Figure 31. IL-1β mRNA expression in WT non-exposed, WT PBS-treated and NECA-treated mice periradicular lesions showing IL-1β gene expression fold change relative to beta actin housekeeping gene. *(n = 10, *P < 0.05 / **P < 0.01).*

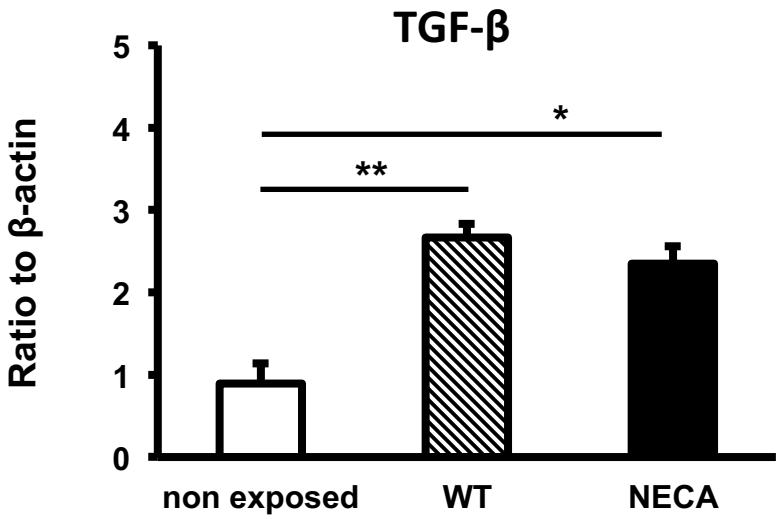

Figure 32. TGF-β mRNA expression in WT non-exposed, WT PBS-treated and NECA-treated mice periradicular lesions showing TGF-β gene expression fold change relative to beta actin housekeeping gene. *(n = 10, *P < 0.05 / **P < 0.01).*

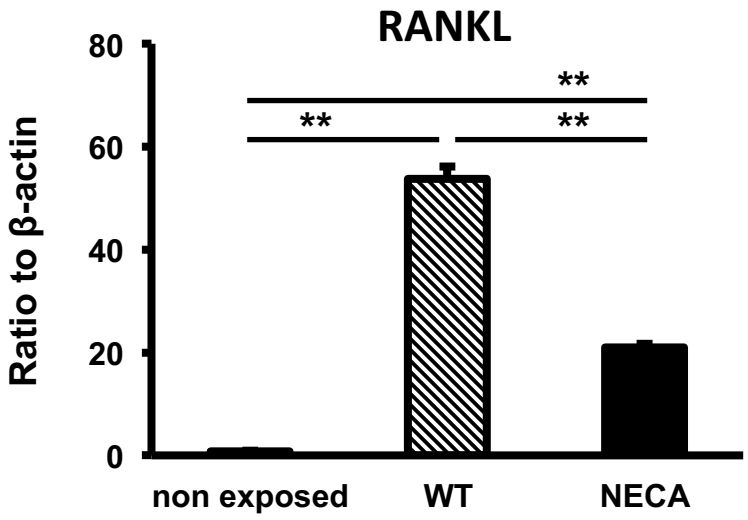

Figure 33. RANKL mRNA expression in WT non-exposed, WT PBS-treated and NECA-treated mice periradicular lesions showing RANKL gene expression fold change relative to beta actin housekeeping gene. *(n = 10, *P < 0.05 / **P < 0.01).*

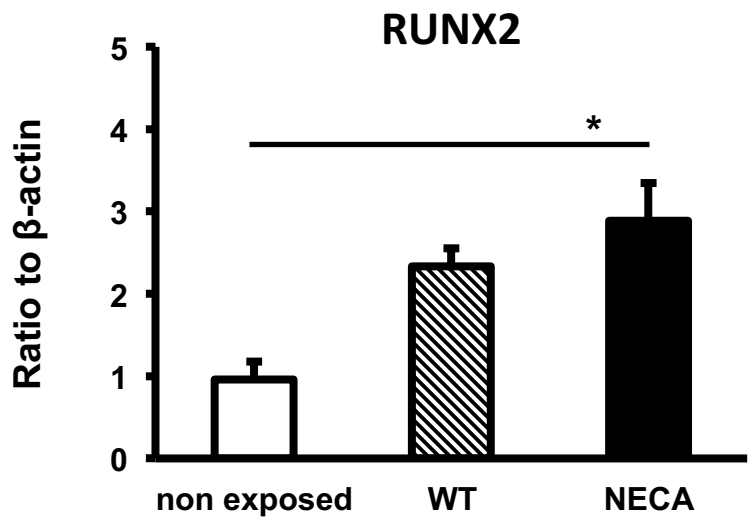

Figure 34. RUNX2 mRNA expression in WT non-exposed, WT PBS-treated and NECA-treated mice periradicular lesions showing RUNX2 gene expression fold change relative to beta actin housekeeping gene. *(n = 10, *P < 0.05 / **P < 0.01).*

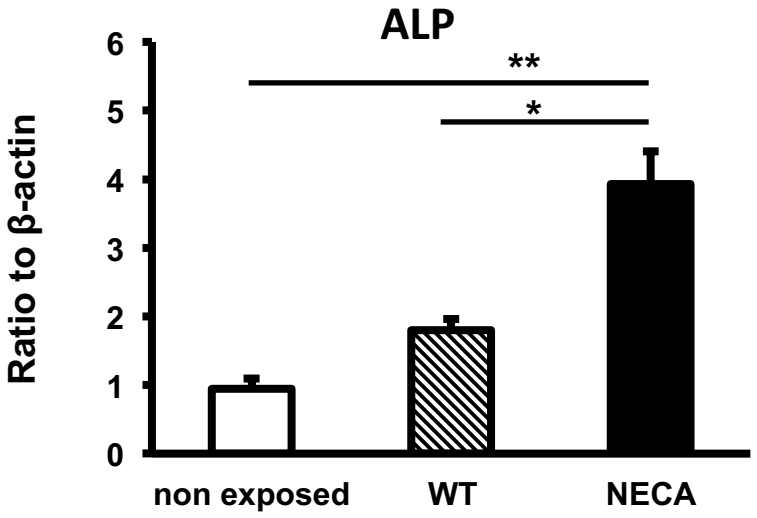

Figure 35. ALP mRNA expression in WT non-exposed, WT PBS-treated and NECA-treated mice periradicular lesions showing ALP gene expression fold change relative to beta actin housekeeping gene. *(n = 10, *P < 0.05 / **P < 0.01).*

References:

1. Kakehashi, S., H.R. Stanley, and R.J. Fitzgerald, *The effects of surgical exposures of dental pulps in germ-free and conventional laboratory rats.* Oral Surg Oral Med Oral Pathol, 1965. **20**: p. 340-9.
2. Sundqvist, *Bacteriological studies of necrotic dental pulp.* The Dental cosmos, 1976. **36:505-528**.
3. Moller, A.J., et al., *Influence on periapical tissues of indigenous oral bacteria and necrotic pulp tissue in monkeys.* Scand J Dent Res, 1981. **89**(6): p. 475-84.
4. Hojo, S., N. Takahashi, and T. Yamada, *Acid profile in carious dentin.* J Dent Res, 1991. **70**(3): p. 182-6.
5. Cameron, C.E., *CRACKED-TOOTH SYNDROME.* J Am Dent Assoc, 1964. **68**: p. 405-11.
6. Nair, P.N., *Apical periodontitis: a dynamic encounter between root canal infection and host response.* Periodontol 2000, 1997. **13**: p. 121-48.
7. Stashenko, P., R. Teles, and R. D'Souza, *Periapical inflammatory responses and their modulation.* Crit Rev Oral Biol Med, 1998. **9**(4): p. 498-521.
8. Teitelbaum, S.L., *Bone resorption by osteoclasts.* Science, 2000. **289**(5484): p. 1504-8.
9. Stashenko, P., S.M. Yu, and C.Y. Wang, *Kinetics of immune cell and bone resorptive responses to endodontic infections.* J Endod, 1992. **18**(9): p. 422-6.
10. Nair, P.N., *Pathogenesis of apical periodontitis and the causes of endodontic failures.* Crit Rev Oral Biol Med, 2004. **15**(6): p. 348-81.
11. Sjogren, U., et al., *Factors affecting the long-term results of endodontic treatment.* J Endod, 1990. **16**(10): p. 498-504.
12. Kawashima, N., et al., *Kinetics of macrophages and lymphoid cells during the development of experimentally induced periapical lesions in rat molars: a quantitative immunohistochemical study.* J Endod, 1996. **22**(6): p. 311-6.
13. Marton, I.J. and C. Kiss, *Characterization of inflammatory cell infiltrate in dental periapical lesions.* Int Endod J, 1993. **26**(2): p. 131-6.
14. Stern, M.H., et al., *Quantitative analysis of cellular composition of human periapical granuloma.* J Endod, 1981. **7**(3): p. 117-22.
15. Stern, M.H., et al., *Isolation and characterization of inflammatory cells from the human periapical granuloma.* J Dent Res, 1982. **61**(12): p. 1408-12.
16. Torabinejad, M. and J.D. Kettering, *Identification and relative concentration of B and T lymphocytes in human chronic periapical lesions.* J Endod, 1985. **11**(3): p. 122-5.

17. Stashenko, P., *Role of immune cytokines in the pathogenesis of periapical lesions.* Endod Dent Traumatol, 1990. **6**(3): p. 89-96.
18. Medzhitov, R. and C. Janeway, Jr., *Innate immunity.* N Engl J Med, 2000. **343**(5): p. 338-44.
19. Yasuda, H., et al., *Osteoclast differentiation factor is a ligand for osteoprotegerin/osteoclastogenesis-inhibitory factor and is identical to TRANCE/RANKL.* Proc Natl Acad Sci U S A, 1998. **95**(7): p. 3597-602.
20. Lacey, D.L., et al., *Osteoprotegerin ligand is a cytokine that regulates osteoclast differentiation and activation.* Cell, 1998. **93**(2): p. 165-76.
21. Boyce, B.F. and L. Xing, *Biology of RANK, RANKL, and osteoprotegerin.* Arthritis Res Ther, 2007. **9 Suppl 1**: p. S1.
22. Kong, Y.Y., et al., *OPGL is a key regulator of osteoclastogenesis, lymphocyte development and lymph-node organogenesis.* Nature, 1999. **397**(6717): p. 315-23.
23. Hofbauer, L.C., C.A. Kuhne, and V. Viereck, *The OPG/RANKL/RANK system in metabolic bone diseases.* J Musculoskelet Neuronal Interact, 2004. **4**(3): p. 268-75.
24. Kawashima, N., et al., *Kinetics of RANKL, RANK and OPG expressions in experimentally induced rat periapical lesions.* Oral Surg Oral Med Oral Pathol Oral Radiol Endod, 2007. **103**(5): p. 707-11.
25. Vernal, R., et al., *RANKL in human periapical granuloma: possible involvement in periapical bone destruction.* Oral Dis, 2006. **12**(3): p. 283-9.
26. Gershon, R.K. and K. Kondo, *Cell interactions in the induction of tolerance: the role of thymic lymphocytes.* Immunology, 1970. **18**(5): p. 723-37.
27. Sakaguchi, S., et al., *Immunologic self-tolerance maintained by activated T cells expressing IL-2 receptor alpha-chains (CD25). Breakdown of a single mechanism of self-tolerance causes various autoimmune diseases.* J Immunol, 1995. **155**(3): p. 1151-64.
28. Thornton, A.M. and E.M. Shevach, *CD4+CD25+ immunoregulatory T cells suppress polyclonal T cell activation in vitro by inhibiting interleukin 2 production.* J Exp Med, 1998. **188**(2): p. 287-96.
29. Shevach, E.M., *CD4+ CD25+ suppressor T cells: more questions than answers.* Nat Rev Immunol, 2002. **2**(6): p. 389-400.
30. Serra, P., et al., *CD40 ligation releases immature dendritic cells from the control of regulatory CD4+CD25+ T cells.* Immunity, 2003. **19**(6): p. 877-89.
31. Cederbom, L., H. Hall, and F. Ivars, *CD4+CD25+ regulatory T cells down-regulate co-stimulatory molecules on antigen-presenting cells.* Eur J Immunol, 2000. **30**(6): p. 1538-43.

32. Takahashi, T., et al., *Immunologic self-tolerance maintained by CD25+CD4+ naturally anergic and suppressive T cells: induction of autoimmune disease by breaking their anergic/suppressive state.* Int Immunol, 1998. **10**(12): p. 1969-80.

33. Silva, M.J., et al., *Bacteria-reactive immune response may induce RANKL-expressing T cells in the mouse periapical bone loss lesion.* J Endod, 2012. **38**(3): p. 346-50.

34. Nakajima, T., et al., *Regulatory T-cells infiltrate periodontal disease tissues.* J Dent Res, 2005. **84**(7): p. 639-43.

35. Ernst, C.W., et al., *Diminished forkhead box P3/CD25 double-positive T regulatory cells are associated with the increased nuclear factor-kappaB ligand (RANKL+) T cells in bone resorption lesion of periodontal disease.* Clin Exp Immunol, 2007. **148**(2): p. 271-80.

36. Cardoso, C.R., et al., *Characterization of CD4+CD25+ natural regulatory T cells in the inflammatory infiltrate of human chronic periodontitis.* J Leukoc Biol, 2008. **84**(1): p. 311-8.

37. Colic, M., et al., *Regulatory T-cells in periapical lesions.* J Dent Res, 2009. **88**(11): p. 997-1002.

38. Colic, M., et al., *Proinflammatory and immunoregulatory mechanisms in periapical lesions.* Mol Immunol, 2009. **47**(1): p. 101-13.

39. AlShwaimi, E., et al., *Regulatory T cells in mouse periapical lesions.* J Endod, 2009. **35**(9): p. 1229-33.

40. Thompson, L.F., et al., *Crucial role for ecto-5'-nucleotidase (CD73) in vascular leakage during hypoxia.* J Exp Med, 2004. **200**(11): p. 1395-405.

41. Mandapathil, M., et al., *Isolation of functional human regulatory T cells (Treg) from the peripheral blood based on the CD39 expression.* J Immunol Methods, 2009. **346**(1-2): p. 55-63.

42. Schuler, P.J., et al., *Separation of human CD4+CD39+ T cells by magnetic beads reveals two phenotypically and functionally different subsets.* J Immunol Methods, 2011. **369**(1-2): p. 59-68.

43. Antonioli, L., et al., *CD39 and CD73 in immunity and inflammation.* Trends Mol Med, 2013. **19**(6): p. 355-67.

44. Romio, M., et al., *Extracellular purine metabolism and signaling of CD73-derived adenosine in murine Treg and Teff cells.* Am J Physiol Cell Physiol, 2011. **301**(2): p. C530-9.

45. Eltzschig, H.K., C.F. Macmanus, and S.P. Colgan, *Neutrophils as sources of extracellular nucleotides: functional consequences at the vascular interface.* Trends Cardiovasc Med, 2008. **18**(3): p. 103-7.

46. Pulte, E.D., et al., *CD39/NTPDase-1 activity and expression in normal leukocytes.* Thromb Res, 2007. **121**(3): p. 309-17.

47. Flogel, U., et al., *Selective activation of adenosine A2A receptors on immune cells by a CD73-dependent prodrug suppresses joint inflammation in experimental rheumatoid arthritis.* Sci Transl Med, 2012. **4**(146): p. 146ra108.

48. Linden, J., *Cell biology. Purinergic chemotaxis.* Science, 2006. **314**(5806): p. 1689-90.

49. Levesque, S.A., et al., *NTPDase1 governs P2X7-dependent functions in murine macrophages.* Eur J Immunol, 2010. **40**(5): p. 1473-85.

50. Hasko, G., et al., *Ecto-5'-nucleotidase (CD73) decreases mortality and organ injury in sepsis.* J Immunol, 2011. **187**(8): p. 4256-67.

51. Petrovic-Djergovic, D., et al., *Tissue-resident ecto-5' nucleotidase (CD73) regulates leukocyte trafficking in the ischemic brain.* J Immunol, 2012. **188**(5): p. 2387-98.

52. Zanin, R.F., et al., *Differential macrophage activation alters the expression profile of NTPDase and ecto-5'-nucleotidase.* PLoS One, 2012. **7**(2): p. e31205.

53. Csoka, B., et al., *Adenosine promotes alternative macrophage activation via A2A and A2B receptors.* FASEB J, 2012. **26**(1): p. 376-86.

54. Schulte, G. and B.B. Fredholm, *The G(s)-coupled adenosine A(2B) receptor recruits divergent pathways to regulate ERK1/2 and p38.* Exp Cell Res, 2003. **290**(1): p. 168-76.

55. Evans, B.A., et al., *Human osteoblast precursors produce extracellular adenosine, which modulates their secretion of IL-6 and osteoprotegerin.* J Bone Miner Res, 2006. **21**(2): p. 228-36.

56. Khakh, B.S. and R.A. North, *P2X receptors as cell-surface ATP sensors in health and disease.* Nature, 2006. **442**(7102): p. 527-32.

57. Brown, R.M. and J.L. Short, *Adenosine A(2A) receptors and their role in drug addiction.* J Pharm Pharmacol, 2008. **60**(11): p. 1409-30.

58. Gessi, S., et al., *Adenosine receptor targeting in health and disease.* Expert Opin Investig Drugs, 2011. **20**(12): p. 1591-609.

59. Korcok, J., et al., *Extracellular nucleotides act through P2X7 receptors to activate NF-kappaB in osteoclasts.* J Bone Miner Res, 2004. **19**(4): p. 642-51.

60. Korcok, J., et al., *P2Y6 nucleotide receptors activate NF-kappaB and increase survival of osteoclasts.* J Biol Chem, 2005. **280**(17): p. 16909-15.

61. Rath-Wolfson, L., et al., *IB-MECA, an A3 adenosine receptor agonist prevents bone resorption in rats with adjuvant induced arthritis.* Clin Exp Rheumatol, 2006. **24**(4): p. 400-6.

62. Kontiainen, S., H. Ranta, and I. Lautenschlager, *Cells infiltrating human periapical inflammatory lesions.* J Oral Pathol, 1986. **15**(10): p. 544-6.

63. Deaglio, S., et al., *Adenosine generation catalyzed by CD39 and CD73 expressed on regulatory T cells mediates immune suppression.* J Exp Med, 2007. **204**(6): p. 1257-65.

64. Scheibner, K.A., et al., *The adenosine a2a receptor inhibits matrix-induced inflammation in a novel fashion.* Am J Respir Cell Mol Biol, 2009. **40**(3): p. 251-9.

65. Ring, S., A.H. Enk, and K. Mahnke, *Regulatory T cells from IL-10-deficient mice fail to suppress contact hypersensitivity reactions due to lack of adenosine production.* J Invest Dermatol, 2011. **131**(7): p. 1494-502.

66. Kawai, T., et al., *Cross-reactive adaptive immune response to oral commensal bacteria results in an induction of receptor activator of nuclear factor-kappaB ligand (RANKL)-dependent periodontal bone resorption in a mouse model.* Oral Microbiol Immunol, 2007. **22**(3): p. 208-15.

67. Balto, K., et al., *Quantification of periapical bone destruction in mice by micro-computed tomography.* J Dent Res, 2000. **79**(1): p. 35-40.

68. da Silva, R.A., et al., *Toll-like receptor 2 knockout mice showed increased periapical lesion size and osteoclast number.* J Endod, 2012. **38**(6): p. 803-13.

69. de Oliveira Rde, C., et al., *Higher expression of galectin-3 and galectin-9 in periapical granulomas than in radicular cysts and an increased toll-like receptor-2 and toll-like receptor-4 expression are associated with reactivation of periapical inflammation.* J Endod, 2014. **40**(2): p. 199-203.

70. Desai, S.V., et al., *Toll-like receptor 2 expression in refractory periapical lesions.* Int Endod J, 2011. **44**(10): p. 907-16.

71. Zhu, Q., *A review of novel bacterial complex lipids: implications for the pathogenesis of apical periodontitis.* Iran Endod J, 2010. **5**(4): p. 141-6.

72. Baik, J.E., et al., *Lipoteichoic acid partially contributes to the inflammatory responses to Enterococcus faecalis.* J Endod, 2008. **34**(8): p. 975-82.

73. Yang, H., et al., *MD-2 is required for disulfide HMGB1-dependent TLR4 signaling.* J Exp Med, 2015. **212**(1): p. 5-14.

74. Tsai, S.Y., et al., *DAMP molecule S100A9 acts as a molecular pattern to enhance inflammation during influenza A virus infection: role of DDX21-TRIF-TLR4-MyD88 pathway.* PLoS Pathog, 2014. **10**(1): p. e1003848.

75. Cunha, C., et al., *DAMP signaling in fungal infections and diseases.* Front Immunol, 2012. **3**: p. 286.

76. Pisetsky, D.S., *The role of nuclear macromolecules in innate immunity.* Proc Am Thorac Soc, 2007. **4**(3): p. 258-62.

77. Heil, M. and W.G. Land, *Danger signals - damaged-self recognition across the tree of life.* Front Plant Sci, 2014. **5**: p. 578.

78. Medina-Castellanos, E., et al., *Extracellular ATP activates MAPK and ROS signaling during injury response in the fungus Trichoderma atroviride.* Front Plant Sci, 2014. **5**: p. 659.

79. Johnson, L., et al., *Porphyromonas gingivalis attenuates ATP-mediated inflammasome activation and HMGB1 release through expression of a nucleoside-diphosphate kinase.* Microbes Infect, 2015. **17**(5): p. 369-77.

80. Spildrejorde, M., et al., *Extracellular adenosine 5'-triphosphate and lipopolysaccharide induce interleukin-1beta release in canine blood.* Vet Immunol Immunopathol, 2014. **157**(1-2): p. 105-10.

81. Azuma, M.M., et al., *The role of IL-6 on apical periodontitis: a systematic review.* Int Endod J, 2014. **47**(7): p. 615-21.

82. Hernadi, K., et al., *Elevated tumor necrosis factor-alpha expression in periapical lesions infected by Epstein-Barr virus.* J Endod, 2013. **39**(4): p. 456-60.

83. de Brito, L.C., et al., *T-lymphocyte and cytokine expression in human inflammatory periapical lesions.* J Endod, 2012. **38**(4): p. 481-5.

84. Fan, R., et al., *Receptor activator of nuclear factor kappa B ligand and osteoprotegerin expression in chronic apical periodontitis: possible association with inflammatory cells.* Chin Med J (Engl), 2011. **124**(14): p. 2162-6.

85. Teixeira-Salum, T.B., et al., *Distinct Th1, Th2 and Treg cytokines balance in chronic periapical granulomas and radicular cysts.* J Oral Pathol Med, 2010. **39**(3): p. 250-6.

86. Ihan Hren, N., et al., *Immune response in chronic periapical parodonititis.* Pflugers Arch, 2000. **440**(5 Suppl): p. R86-8.

87. Katebzadeh, N., J. Hupp, and M. Trope, *Histological periapical repair after obturation of infected root canals in dogs.* J Endod, 1999. **25**(5): p. 364-8.

88. Tanomaru Filho, M., M.R. Leonardo, and L.A. da Silva, *Effect of irrigating solution and calcium hydroxide root canal dressing on the repair of apical and periapical tissues of teeth with periapical lesion.* J Endod, 2002. **28**(4): p. 295-9.

89. Vera, J., et al., *One- versus two-visit endodontic treatment of teeth with apical periodontitis: a histobacteriologic study.* J Endod, 2012. **38**(8): p. 1040-52.

90. Bono, M.R., et al., *CD73 and CD39 ectonucleotidases in T cell differentiation: Beyond immunosuppression.* FEBS Lett, 2015.

91. Alam, M.S., et al., *Extracellular adenosine generation in the regulation of pro-inflammatory responses and pathogen colonization.* Biomolecules, 2015. **5**(2): p. 775-92.

92. Feng, L., et al., *Vascular CD39/ENTPD1 directly promotes tumor cell growth by scavenging extracellular adenosine triphosphate.* Neoplasia, 2011. **13**(3): p. 206-16.

93. Kas-Deelen, A.M., et al., *Cytomegalovirus infection increases the expression and activity of ecto-ATPase (CD39) and ecto-5'nucleotidase (CD73) on endothelial cells.* FEBS Lett, 2001. **491**(1-2): p. 21-5.

94. Nikolova, M., et al., *CD39/adenosine pathway is involved in AIDS progression.* PLoS Pathog, 2011. **7**(7): p. e1002110.

95. Schuler, P.J., et al., *CD4(+)CD73(+) T cells are associated with lower T-cell activation and C reactive protein levels and are depleted in HIV-1 infection regardless of viral suppression.* AIDS, 2013. **27**(10): p. 1545-55.

96. Peres, R.S., et al., *Low expression of CD39 on regulatory T cells as a biomarker for resistance to methotrexate therapy in rheumatoid arthritis.* Proc Natl Acad Sci U S A, 2015. **112**(8): p. 2509-14.

97. Fletcher, J.M., et al., *CD39+Foxp3+ regulatory T Cells suppress pathogenic Th17 cells and are impaired in multiple sclerosis.* J Immunol, 2009. **183**(11): p. 7602-10.

98. Rajasekaran, N., et al., *B6.g7 mice reconstituted with BDC2.5 non-obese diabetic (BDC2.5NOD) stem cells do not develop autoimmune diabetes.* Clin Exp Immunol, 2013. **174**(1): p. 27-37.

99. Sacktor, B., *Sodium-coupled hexose transport.* Kidney Int, 1989. **36**(3): p. 342-50.

100. Hasib, L., et al., *Functional and homeostatic defects of regulatory T cells in patients with coronary artery disease.* J Intern Med, 2016. **279**(1): p. 63-77.

101. Xia, N., et al., *Activated regulatory T-cells attenuate myocardial ischaemia/reperfusion injury through a CD39-dependent mechanism.* Clin Sci (Lond), 2015. **128**(10): p. 679-93.

102. Sun, X., et al., *CD39/ENTPD1 expression by CD4+Foxp3+ regulatory T cells promotes hepatic metastatic tumor growth in mice.* Gastroenterology, 2010. **139**(3): p. 1030-40.

103. Mediero, A. and B.N. Cronstein, *Adenosine and bone metabolism.* Trends Endocrinol Metab, 2013. **24**(6): p. 290-300.

104. Kawai, T., et al., *B and T lymphocytes are the primary sources of RANKL in the bone resorptive lesion of periodontal disease.* Am J Pathol, 2006. **169**(3): p. 987-98.

105. Hao, L., et al., *A small molecule, odanacatib, inhibits inflammation and bone loss caused by endodontic disease.* Infect Immun, 2015. **83**(4): p. 1235-45.

106. Xiong, H., et al., *Effect of alendronate on alveolar bone resorption and angiogenesis in rats with experimental periapical lesions.* Int Endod J, 2010. **43**(6): p. 485-91.

107. Ma, J., et al., *RNA interference-mediated silencing of Atp6i prevents both periapical bone erosion and inflammation in the mouse model of endodontic disease.* Infect Immun, 2013. **81**(4): p. 1021-30.

108. de Molon, R.S., et al., *Spontaneous osteonecrosis of the jaws in the maxilla of mice on antiresorptive treatment: a novel ONJ mouse model.* Bone, 2014. **68**: p. 11-9.

109. Preti, D., et al., *History and perspectives of A2A adenosine receptor antagonists as potential therapeutic agents.* Med Res Rev, 2015. **35**(4): p. 790-848.

110. Yuan, G. and G.B. Jones, *Towards next generation adenosine A(2A) receptor antagonists.* Curr Med Chem, 2014. **21**(34): p. 3918-35.

111. !!! INVALID CITATION !!!

112. Kinsey, G.R., et al., *Autocrine adenosine signaling promotes regulatory T cell-mediated renal protection.* J Am Soc Nephrol, 2012. **23**(9): p. 1528-37.

113. Ohta, A., et al., *The development and immunosuppressive functions of CD4(+) CD25(+) FoxP3(+) regulatory T cells are under influence of the adenosine-A2A adenosine receptor pathway.* Front Immunol, 2012. **3**: p. 190.

114. Mills, J.H., et al., *A2A adenosine receptor signaling in lymphocytes and the central nervous system regulates inflammation during experimental autoimmune encephalomyelitis.* J Immunol, 2012. **188**(11): p. 5713-22.

115. Rui, L., *Energy metabolism in the liver.* Compr Physiol, 2014. **4**(1): p. 177-97.

116. Gorini, S., et al., *Regulation of innate immunity by extracellular nucleotides.* Am J Blood Res, 2013. **3**(1): p. 14-28.

117. Jacobson, K.A. and C.E. Muller, *Medicinal chemistry of adenosine, P2Y and P2X receptors.* Neuropharmacology, 2015.

118. North, R.A. and M.F. Jarvis, *P2X receptors as drug targets.* Mol Pharmacol, 2013. **83**(4): p. 759-69.

119. Morandini, A.C., L.E. Savio, and R. Coutinho-Silva, *The role of P2X7 receptor in infectious inflammatory diseases and the influence of ectonucleotidases.* Biomed J, 2014. **37**(4): p. 169-77.

120. Kawamura, H., et al., *Extracellular ATP-stimulated macrophages produce macrophage inflammatory protein-2 which is important for neutrophil migration.* Immunology, 2012. **136**(4): p. 448-58.

121. Hong, S., et al., *Differential regulation of P2X7 receptor activation by extracellular nicotinamide adenine dinucleotide and ecto-ADP-ribosyltransferases in murine macrophages and T cells.* J Immunol, 2009. **183**(1): p. 578-92.

122. Okiji, T., et al., *Distribution of Ia antigen-expressing nonlymphoid cells in various stages of induced periapical lesions in rat molars.* J Endod, 1994. **20**(1): p. 27-31.

123. Akamine, A., et al., *Immunohistochemical examination on the localization of macrophages and plasma cells in induced rat periapical lesions.* Endod Dent Traumatol, 1994. **10**(3): p. 121-8.

124. Huang, G.T., et al., *Effect of interleukin-6 deficiency on the formation of periapical lesions after pulp exposure in mice.* Oral Surg Oral Med Oral Pathol Oral Radiol Endod, 2001. **92**(1): p. 83-8.

125. Borsellino, G., et al., *Expression of ectonucleotidase CD39 by Foxp3+ Treg cells: hydrolysis of extracellular ATP and immune suppression.* Blood, 2007. **110**(4): p. 1225-32.

126. Alam, M.S., et al., *CD73 is expressed by human regulatory T helper cells and suppresses proinflammatory cytokine production and Helicobacter felis-induced gastritis in mice.* J Infect Dis, 2009. **199**(4): p. 494-504.

127. Ryzhov, S., et al., *Effect of A2B adenosine receptor gene ablation on adenosine-dependent regulation of proinflammatory cytokines.* J Pharmacol Exp Ther, 2008. **324**(2): p. 694-700.

128. Regateiro, F.S., et al., *Generation of anti-inflammatory adenosine by leukocytes is regulated by TGF-beta.* Eur J Immunol, 2011. **41**(10): p. 2955-65.

129. Luckprom, P., et al., *Adenosine triphosphate stimulates RANKL expression through P2Y1 receptor-cyclo-oxygenase-dependent pathway in human periodontal ligament cells.* J Periodontal Res, 2010. **45**(3): p. 404-11.

130. Buckley, K.A., et al., *Adenosine triphosphate stimulates human osteoclast activity via upregulation of osteoblast-expressed receptor activator of nuclear factor-kappa B ligand.* Bone, 2002. **31**(5): p. 582-90.

131. Lim, J.C. and C.H. Mitchell, *Inflammation, pain, and pressure--purinergic signaling in oral tissues.* J Dent Res, 2012. **91**(12): p. 1103-9.

132. Takedachi, M., et al., *CD73-generated adenosine promotes osteoblast differentiation.* J Cell Physiol, 2012. **227**(6): p. 2622-31.

133. Evans, B.A., *Does adenosine play a role in bone formation, resorption and repair?* Purinergic Signal, 2012. **8**(2): p. 177-80.

134. Orriss, I.R., et al., *Osteoblast responses to nucleotides increase during differentiation.* Bone, 2006. **39**(2): p. 300-9.